Regulation of tissue healing by the extracellular matrix

AALBORG UNIVERSITY
DENMARK

In collaboration with the Cardiology Stem Cell Center, Rigshospitalet

Master thesis by

Camilla Lyngsøe Østergaard & Emma Bust Gravesen

Medicine with Industrial Specialization, Biomedicine

9 and 10th semester, Autumn 2021 - Spring 2022, Aalborg University

AALBORG UNIVERSITET

Department of Health Science and Technology

Medicine with Industrial Specialization, Biomedicine

Title:

Regulation of tissue healing by the extracellular matrix

Semester:

9 and 10th semester

Project period:

Autumn 2021 - Spring 2022

ECTS:

60

Group number:

9042

Supervisor:

Cristian Pablo Pennisi

Co-supervisor:

Morten Juhl

Participants:

Camilla Lyngsøe Østergaard

Emma Bust Gravesen

Pages:

42

Appendix:

24 pages

Acknowledgments

We would like to thank our supervisor Cristian Pablo Pennisi for his time and dedication throughout this project, and the regenerative medicine group for letting us participate in meetings and seek counsel.

A special thanks to the Cardiology Stem Cell Center at Rigshospitalet for the collaboration during this master thesis. A special thanks to our co-supervisor Morten Juhl for his engagement and supervision in our project. We would also like to thank Stine Bangsgaard Hansen for her help both in and out of the lab.

Table of contents

List of abbreviations

AB	Antibody
ASCs	Adipose-derived stem cells
BSA	Bovine serum albumin
COL1	Collagen type 1 alpha 1
COL3	Collagen type 3 alpha 1
CS	Chondroitin sulfate
DAMP	Damage-associated molecular patterns
DMEM	Dulbecco's Modified Eagle Medium
EB	Extraction buffer
ECM	Extracellular matrix
FCF	Fetal calf serum
FGF	Fibroblast growth factor
FVO	Fractional volume occupancy
GAG	Glycosaminoglycan
GF	Growth factor
GM-CSF	Granulocyte-macrophage colony-stimulating factor
GOI	Gene of interest
HA	Hyaluronan
HAS2	Hyaluronan synthase 2
IFN-γ	Interferon-gamma
iM2	Immature M2
iM2	Immature M2
LPS	Lipopolysaccharide
M-CSF	Macrophage colony-stimulating factor
MACS	Magnetic-activated cell sorting
MHC II	Major histocompatibility complex class II
Mins	Minutes
mM1	Mature M1
MMP1	Matrix metalloproteinase 1
MMP2	Matrix metalloproteinase 2
MMPs	Matrix metalloproteinases
MSC	Mesenchymal stem cell
OD	Optical density
PAMP	Pathogen-specific molecular patterns
PBMCs	Peripheral blood mononuclear cells.
PBS	Phosphate-buffered saline
PDGF	Platelet-derived growth factor
PDGF-R	Platelet-derived growth factor receptor
PMNs	Polymorphonuclear leukocytes
PPIA	Peptidylprolyl Isomerase A
qPCR	Quantitative polymerase chain reaction
RPM	Rounds per minute
RT	Room temperature
sGAG	Sulfated glycosaminoglycans
SR/FG	Sirius Red/Fast Green
TGF-β	Transforming growth factor β
TIMPs	Tissue inhibitor metalloproteinases

English abstract

Introduction: The wound healing process consists of different phases relying on many factors and processes, which can be disturbed and lead to insufficient healing. The extracellular matrix (ECM) and macrophages have a key role in the wound healing process. It is known that adipose-derived stem cells (ASCs) share several features with fibroblasts. Therefore, this study will compare the ECM produced by fibroblasts and ASCs, and the ability of ECM to modulate the behavior- and immunophenotype of macrophages.

Methods: Human ASCs and -foreskin fibroblasts were cultured under conditions that promoted ECM deposition. Quantitative polymerase chain reaction (qPCR) was performed on ECM-related genes: *COL1, COL3, FIB*, *MMP1, MMP2, TIMP1,* and *HAS2* of ASCs and fibroblasts. After decellularization, immunofluorescence was used to assess the deposition of collagen I and -III, fibronectin, laminin, and chondroitin sulfate (CS). Sirius Red/Fast Green (SR/FG) was performed to assess collagen deposition in the ECM. CD14+ monocytes were polarized into iM1, mM1, iM2, and M2c and seeded on ECM. Picrosirius red was performed, and surface marker expression was assessed by flow cytometry.

Results: As compared to fibroblast ECM, higher levels of collagen, non-collagenous proteins, and sulfated glycosaminoglycans (sGAGs) were found in ASC ECM. While fibronectin, collagen I and -III, and CS expression was higher in fibroblast ECM, more laminin was found in ASC ECM. The relative gene expression (RGE) of *COL1, COL3, FIB, MMP2, TIMP1,* and *HAS2* was higher in ASCs than in fibroblasts. The RGE of MMP1 was lower in ASCs than in fibroblasts on day one. Morphological differences between iM1, iM2, mM1, and M2c were observed and picrosirius red revealed elongated mM1 and M2c along the ECM. iM1 and mM1 were HLA-DR+, CD86+, CD206+, and CD68+, though mM1 was also CD38+ and ILT4+. iM2 and M2c were CD14+, CD68+, CD163+, CD86+, and ILT4+.

Conclusion: The observed differences in transcriptional activity and expression of ECM components suggest that ASCs exhibit a greater ability to deposit ECM than fibroblasts. Morphological changes were observed, and expression of surface markers could indicate that ASC ECM, in contrast to fibroblasts ECM, influences macrophages toward a less pro-inflammatory phenotype, suggesting a possible immunomodulatory effect of ASC ECM.

Dansk abstract

Introduktion: Sårhelingsprocessen består af forskellige faser som indeholder mange faktorer og processer, hvilke kan forstyrres og dermed føre til utilstrækkelig sårheling. Den ekstracellulære matrix (ECM) og makrofager har en vigtig rolle i sårhelingsprocessen. Det vides at adipøse stamceller (ASC'er) har mange funktioner tilfælles med fibroblaster. Derfor vil dette studie sammenligne ECM produceret af fibroblaster og ASC'er og ECM's evne til at modulere adfærd- og immunfænotype af makrofager.

Metode: Humane ASC'er og -forhuds fibroblaster blev dyrket under betingelser, der fremmede ECM-aflejring. Kvantitativ polymerasekædereaktion (qPCR) blev udført på ECM-relaterede gener: *COL1, COL3, FIB, MMP1, MMP2, TIMP1* og *HAS2* af ASC'er og fibroblaster. Efter decellularisering blev immunfluorescens brugt til at vurdere aflejringen af kollagen I og -III, fibronectin, laminin og chondroitinsulfat (CS). Sirius Red/Fast Green (SR/FG) blev udført for at vurdere kollagen aflejring i ECM. CD14+ monocytter blev induceret til iM1, mM1, iM2 og M2c og udsået på ECM. Der blev udført picrosirius rød farvning, og overflademarkør-ekspression blev vurderet ved flowcytometri.

Resultater: Sammenlignet med fibroblast ECM blev der fundet højere niveauer af kollagen, ikke-kollagene proteiner og sulfaterede glycosaminoglycaner (sGAG'er) i ASC ECM. Fibronectin, collagen I og -III og CS ekspression var højere i fibroblast ECM, men blev der fundet mere laminin i ASC ECM. Den relative genekspression (RGE) af *COL1, COL3, FIB, MMP2, TIMP1* og *HAS2* var højere i ASC'er end i fibroblaster. RGE for MMP1 var lavere i ASC'er end i fibroblaster på dag et. Der blev observeret morfologiske forskelle mellem iM1, iM2, mM1 og M2c, og picrosirius rød afslørede aflange mM1 og M2c langs ECM. iM1 og mM1 var HLA-DR+, CD86+, CD206+ og CD68+, dog var mM1 også CD38+ og ILT4+. iM2 og M2c var CD14+, CD68+, CD163+, CD86+ og ILT4+.

Konklusion: Forskellene i transskriptionel aktivitet og ekspression af ECM-komponenter tyder på, at ASC'er udviser større evne til at deponere ECM end fibroblaster. Morfologiske ændringer blev observeret, og ekspression af overflademarkører kunne indikere, at ASC ECM, i modsætning til fibroblast ECM, påvirker makrofager i retning af en mindre proinflammatorisk fænotype, hvilket tyder på en mulig immunmodulerende effekt af ASC ECM.

1 Introduction

In the case of injury to the skin, the healing process commences, which consists of a carefully ordered sequence of events. It consists of overlapping phases, all of which are important for successful wound healing. However, sometimes the healing process can be disturbed resulting in inadequate healing leading to chronic wounds (1).

It is estimated that about 40,000 to 50,000 people in Denmark (2) are treated for chronic wounds each year and chronic wounds are considered to greatly impact the patient's quality of life, as they may induce pain and immobility (3). The problem is however increasing due to a large elder population and an increase in lifestyle diseases such as diabetes (2). Current treatments revolve around dressings and debridement of the wound (1,4); however, they are insufficient, and new therapeutic strategies are necessary (5).

The extracellular matrix (ECM), produced by fibroblasts in the body, is known for its important role in wound healing, by its rapid and dynamic remodeling, and its content of essential growth factors (GF)s. These GFs play an important role in the recruitment and activation of different cells such as macrophages, which are also key regulators of the wound healing process (6,7). Adipose-derived stem cells (ASCs) have also been shown to be able to deposit GFs and structural ECM components essential for the wound healing process, and it is recognized that ASCs also are able to promote the healing of chronic wounds (8). Studies have shown that ASCs share several common features with fibroblasts, including morphology, surface marker expression, differentiation potential, and immunomodulatory properties (9-11). However, the comparison between these two cell types in terms of ECM production and their properties has not been fully elucidated.

Therefore, this study aims to compare the ECM produced by fibroblasts and ASCs, with a special focus on the ability of the ECM to modulate the immunophenotype of macrophages.

1.1 The extracellular matrix (ECM)

The ECM is the non-cellular element present in all tissues, which contributes to a stable structure for maintaining the physical integrity of all cells. It is a dynamic entity that repeatedly undergoes regulated remodeling, and its specific composition is fundamental to

the maintenance of normal tissue function, as it has a big impact on many cellular processes, such as cell proliferation, differentiation, and migration, and is essential for the regenerative ability of the tissue upon injury. The ECM comprises a variety of proteins that can be categorized as structural proteins, such as collagen and elastin, or non-structural proteins, such as glycoproteins and proteoglycans, as illustrated in figure 1. These ECM components are mainly produced by fibroblasts (7).

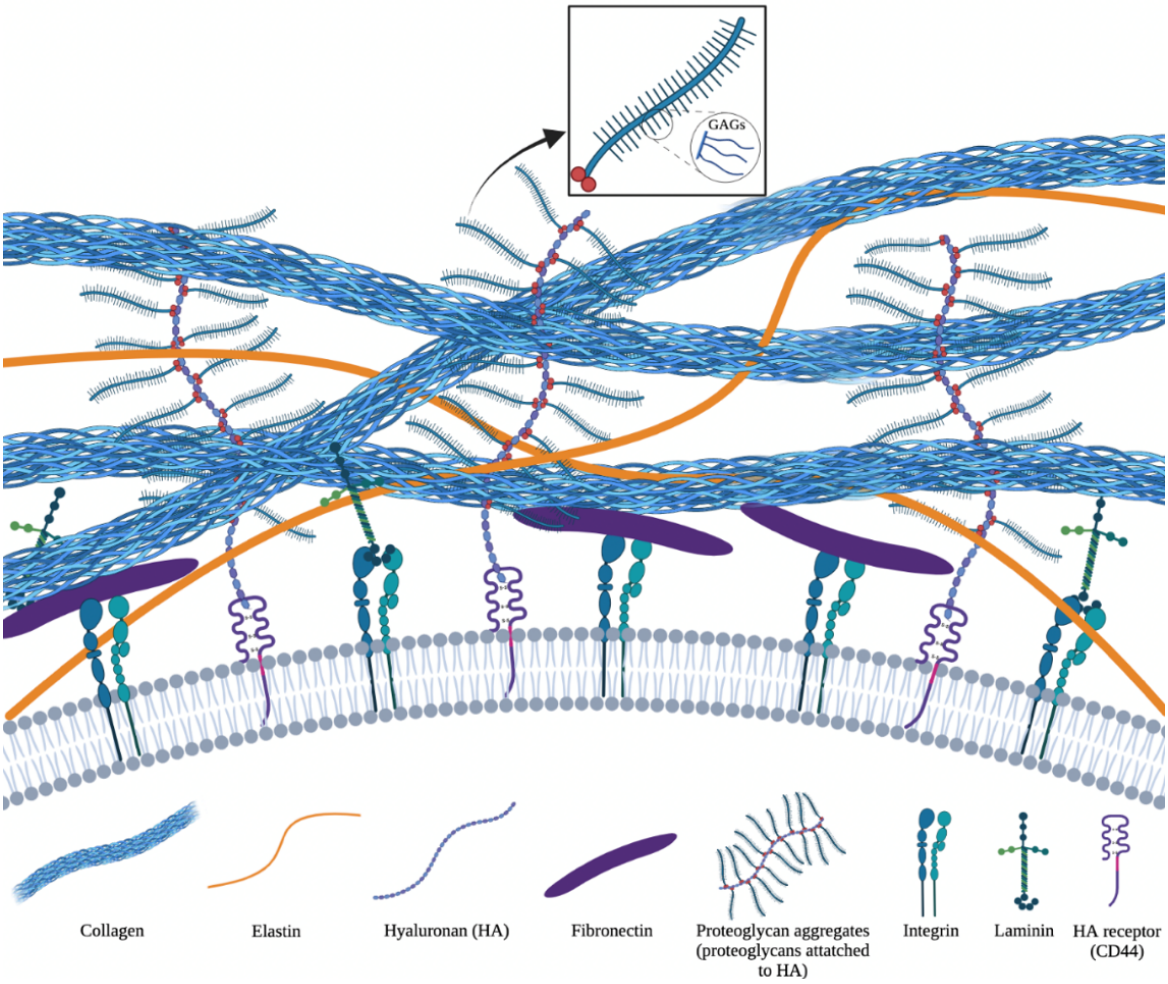

Figure 1: Illustration of ECM including some of the major ECM components and their interactions.

Though there are many types of collagens, the most abundant structural protein in the ECM is collagen I, which is composed of a triple helix arranged into fibrils to provide structural integrity and tensile strength for the tissues, which is necessary to endure mechanical stresses. Additionally, collagen also plays an important role in cell migration and -adhesion (7,12). The production of collagen is regulated by different ECM components, and ascorbic acid, which is an essential co-factor in collagen synthesis (13). Collagen relates to elastin, which is the other structural protein in ECM, as elastin fibers allow tissues to recover when undergoing constant stretching (7,12).

Fibronectin is a glycoprotein formed as disulfide-bonded dimers organized into a fibrillar structure like collagen. Fibronectin is linked to integrins on the cell surface and thus connects cells with other ECM proteins, like collagen. It plays a significant role in the organization of the ECM and mediates different cell processes such as cell adhesion and migration (7,12,14). Another glycoprotein of the ECM is laminin which has a heterotrimeric structure, and, like fibronectin, binds to cells via integrins connecting the basement membrane with the adjoining cell layer. By regulating tissue architecture, cell adhesion, differentiation, migration, and matrix-mediated signaling, laminins play a key role in tissue homeostasis (7,15).

Within the ECM, proteoglycans form a hydrated gel that occupies most of the extracellular interstitial space. Proteoglycans consist of a core protein with one or more covalently attached glycosaminoglycans (GAGs), except for hyaluronan (HA). GAGs are linear negatively charged polysaccharides consisting of repeating disaccharides containing an amino group. They can be categorized into sulfated GAGs, including chondroitin sulfate, dermatan sulfate, heparin, heparan sulfate, and keratan sulfate, and non-sulfated GAGs, such as HA. Due to the hydrophilic nature of these molecules, they provide hydration and adopt highly extensive conformations, enabling the matrix to endure strong compressive forces (12,16,17). The most abundant GAG is chondroitin sulfate, and though it is present throughout the body, it is primarily found in the proteoglycans aggrecan and versican. These proteoglycans are found in the ECM of many tissues, though aggrecan is very abundant in cartilage while versican is found in most soft tissues in the body (18,19). The functions of these proteoglycans are largely governed by their ability to form aggregates, which then contribute to the mechanical properties and signaling functions of the ECM. A very important component essential to aggregate formation is HA, which non-covalently attaches to the proteoglycans, thus organizing the proteoglycans and other ECM proteins. Additionally, proteoglycans bind GFs, thus influencing the signal communication between cells. GFs are abundant in the ECM and can be activated by multiple processes, such as wound healing and ECM remodeling (18-20).

Remodeling of the ECM is a highly regulated process that often is referred to as homeostasis orchestrated by fibroblast matrix metalloproteinases (MMPs) and tissue inhibitors of metalloproteinases (TIMPs) (12). MMPs are enzymes that are involved in the degradation of ECM as they cleave ECM components. It is, however, important to avoid the tissue being degraded too excessively, and therefore TIMPs are important as they inhibit

MMPs. The ratio between MMPs and TIMPs varies, and the proteolytic activity is determined by this variation (21,22).

1.1.2 ASCs

Fibroblasts are not the only cell type to produce ECM components and modulate wound healing. It is known that adipose-derived stem cells (ASCs) also deposit ECM components and GFs which can promote the recovery of damaged tissue. These stem cells are present in the adipose tissue of the body and can easily be obtained through liposuction (8,23). It has been shown that ASC-secreted factors enhance various fibroblast characteristics during the proliferation phase, including cell proliferation, migration, and collagen synthesis. Additionally, they are thought to inhibit ECM degradation and have demonstrated immunomodulatory properties (8).

As described the ECM contains many elements, and it is important that the turnover of these elements is well balanced. If the ECM homeostasis is not well controlled, a continuous dysregulation can lead to severe pathological conditions, such as insufficient wound healing (24).

1.2 Wound healing

Healing of wounds is a complex process that is highly regulated and crucial to maintaining the barrier function of the skin. When an injury occurs, a series of systems are activated at the site of the wound to restore the skin (1). The wound healing process involves interactions between biological and immunological systems and consists of several overlapping phases: the hemostatic phase, the inflammatory phase, the proliferative phase, and the remodeling phase (4,25). The four phases are illustrated in figure 2.

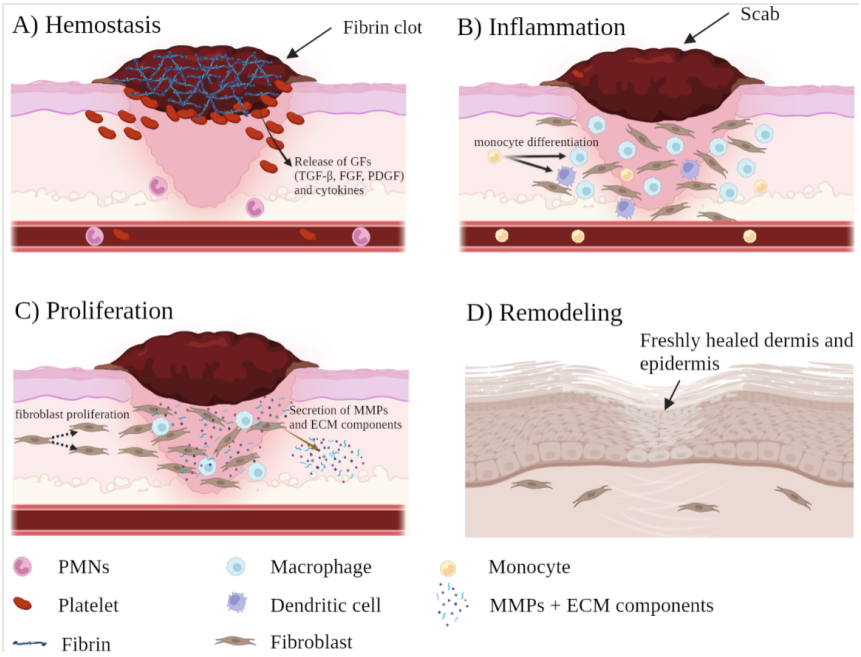

Figure 2 - Illustration of the wound healing process with the four partially overlapping phases. A) Hemostasis: formation of a fibrin clot. B) The inflammatory phase: inflammation and macrophage differentiation with cytokine and GF release. C) The proliferative phase: fibroblast proliferation and secretion of ECM components. D) The remodeling phase: remodeling of ECM.

The first phase, the hemostatic phase, starts immediately after injury with constrictions of vascular structures and the formation of a fibrin clot. The fibrin clot along with the surrounding wound tissue releases GFs and proinflammatory cytokines. Some of the released GFs include transforming growth factor (TGF)-β, fibroblast growth factor (FGF), and platelet-derived growth factor (PDGF) (25,26). In this hemostatic phase, an initial invasion of polymorphonuclear leukocytes (PMNs) occurs when the bleeding is controlled, which characterizes the start of the inflammatory phase (27).

The primary goal of the inflammatory phase is to clear foreign material and pathogens from the wound (1). After the initial invasion of PMNs, monocytes start to infiltrate the wound site and differentiate into macrophages and dendritic cells (27). Macrophages play a key role in the inflammatory phase as they digest and phagocytose tissue debris and neutrophils along with releasing cytokines and GFs that promote cell migration and regeneration of tissue (1).

Following the inflammatory phase is the proliferative phase, which is characterized by the proliferation of fibroblasts and angiogenesis (1). The fibroblasts degrade the fibrin clot by secretion of MMPs and produce collagen, glycosaminoglycans, and proteoglycans which all are important components of the ECM as described earlier. They also produce other ECM components such as HA and heparan sulfate. The matrix formed by the fibroblasts acts as a signal for epithelialization and angiogenesis to occur (1,28). About three

weeks after injury a steady state of collagen synthesis and degradation together with ECM remodeling is reached. MMPs are, as mentioned before, key players in the breakdown of ECM components including collagen, and their activity is regulated tightly by TIMPs. TIMP-activity increases gradually over time and thereby reduces the activity of MMPs resulting in the accumulation of a new intact ECM (4).

The remodeling phase is the last phase in the wound healing process and in this phase, ECM remodeling happens where mature collagen I is formed, and collagen III and profuse ECM is degraded making the ECM more like the architecture of normal tissue (25,26). The remodeling phase results in the closure of the wound and the formation of a collagenous scar (29).

1.2.1 Chronic wounds and treatment

The wound healing process can be disrupted resulting in a halt in the healing process, thus increasing the risk of the wound becoming chronic. The definition of a chronic wound is a wound that has not been able to heal for over three months. This halt in the wound healing process can be caused by several conditions such as trauma and diabetes (5). It is typically in the inflammatory phase the process of wound healing is disrupted resulting in an unbalanced ratio between MMPs and TIMPs. Macrophages are activated in response to the ECM components, and they also play a crucial part in sufficient wound healing. A dysregulated macrophage activation can result in chronic inflammation leading to chronic wounds (8,30).

1.3 Macrophages

As mentioned, macrophages play a major role in the wound healing process and in wound pathology. Macrophages are important in the transformation from the inflammatory phase to the proliferative phase as the absence of macrophages in both phases results in impaired tissue formation and failed progression into the next phase of the wound healing process (29,31).

Macrophages get activated by damage-associated molecular patterns (DAMPs) and pathogen-specific molecular patterns (PAMPs). Early in the wound healing process, this activation of macrophages results in differentiation into M1-type macrophages that are known for their production of pro-inflammatory cytokines. Later, M1-type macrophages transform into M2-type macrophages which are involved in the initiation of fibroblast

proliferation, production of ECM, and synthesis of anti-inflammatory mediators. It has been shown that this transition from the M1-type to the M2-type macrophages is necessary for wounds to heal as no occurrence of this transition results in chronic or nonhealing wounds such as e.g., diabetic wounds (29).

The heterogeneity of macrophages is dependent on the microenvironment surrounding the cells. To heal tissue injury and reduce inflammation, the phenotypic and functional plasticity that macrophages exhibit is of great importance (32,33).

Granulocyte-macrophage colony-stimulating factor (GM-CSF) and macrophage-colony-stimulating factor (M-CSF) are cytokines known to stimulate CD14+ monocytes to differentiate into the immature M1(iM1) and -M2(iM2) phenotypes, respectively (32,33). iM1 macrophages are classically activated by stimulation with lipopolysaccharide (LPS) and interferon (IFN)-γ and the then mature M1 (mM1) are phenotypically characterized by a high expression of CD38 (34), CD86, and major histocompatibility complex class II (MHC II), such as HLA-DR (35-37) as illustrated on figure 3. iM2 macrophages can be polarized into four subtypes: the alternative activated macrophages (M2a), stimulated by IL-4 or IL-13, type 2 macrophages (M2b), activated by immune complexes and LPS, deactivated macrophages (M2c), stimulated by IL-10, TGF-β, and glucocorticoids, and lastly M2d, which can be produced by IL6 and adenosine stimulation (32,37).

Research suggests that the balance between regenerative wound healing and fibrosis, or scar formation, depends on the balance of the cellular functions between the M2a and M2c phenotypes. It has been demonstrated that M2a and M2c both have an important role in tissue healing, as M2a can regulate tissue repair by controlled secretion of TGF-β1 to induce fibroblast differentiation, and M2c can reduce inflammation and facilitate repair processes by secretion of IL-10 (38). The anti-inflammatory M2c phenotype is characterized as CD206+ and CD163+ (32) as illustrated in figure 3.

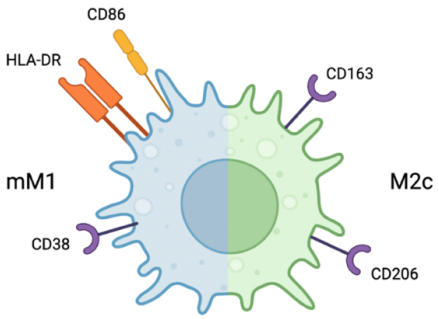

Figure 3 - Illustration of the surface markers on mM1(blue) and M2c(green) macrophages.

1.4 Aim of study

The comparison of the production and properties of ECM derived from ASCs and fibroblasts has not been fully elucidated. Therefore, the aim of this project is to optimize the production of ECM scaffolds and then assess and compare some of the key properties of the ECM deposited by ASCs and fibroblasts in vitro. Furthermore, this study will assess the ability of the ECM to modulate the immunophenotype of macrophages and their behavior on ECM scaffolds.

2 Methods

2.1 Assessment of extracellular matrix (ECM) deposited by human adipose-derived stem cells (ASC)s and human fibroblasts

2.1.1 Cell source and -culture

Two cell types were used in this study: fibroblasts, obtained from human foreskin (CRL2429), and human adipose-derived stem cells (ASCs). The ASCs were isolated from adipose tissue obtained during elective liposuction on a healthy donor. The procedure for the isolation has been described elsewhere along with the ethical protocol approval (5). The same culture medium was used for both cultures of ASCs and fibroblasts and contained: Dulbecco's Modified Eagle Medium (DMEM) (Gibco, Thermo scientific), 10% fetal calf serum (FCS), 100 IU/ml penicillin, and 0.1 mg/ml streptomycin (Thermo scientific). All work involving cells was performed in a LAF-bench class II (Holten Laminair, Denmark).

2.1.1.1 Initiation and maintenance of cell cultures

Cryopreserved fibroblasts and ASCs were thawed in a water bath at 37 °C whereafter they were transferred to a centrifuge tube (one for each cell type). The cells were centrifuged at room temperature (RT) at 1200 RPM for five minutes (mins) before the supernatant was discarded and the pellet resuspended in fresh culture medium. Each cell type was then transferred to a T175 flask and stored in the incubator at 37 °C in 5% CO2 (Thermo Scientific, Steri-Cycle CO2 Incubator). Media change was performed every two to three days. When the cells were confluent in the T175 flask they were either seeded or a cell passage was made. Initially, the cell surface was washed two times with phosphate-buffered saline (PBS) before TrypLE (Gibco) was added to the flask, covering the surface. The flasks were then incubated at 37 °C in 5% CO2 until the cells had detached from the surface of the flask. Culture medium was added to the flask and pipetted up and down a few times to remove any cells remaining on the surface. The medium containing cells was transferred to a centrifuge tube and centrifuged at 1200 RPM for five mins whereafter the supernatant was removed, and the pellet was resuspended in fresh culture medium. The cells were counted using a hemocytometer and the cell concentration was calculated using the following formula:

$$Cell\ concentration \frac{cells}{ml} = average\ cell\ count\ \cdot 10^4$$

From this it is possible to calculate the amount of cell suspension needed to seed cells.

$$Cell\ suspension\ (ml) = \frac{Wanted\ cells\ \left(\frac{cells}{cm^2}\right) \cdot growth\ area\ (cm^2)}{Cell\ concentration \frac{cells}{ml}}$$

2.1.2 Cell seeding and induction of cells for ECM deposition

ASCs and fibroblasts were seeded in sterile 24-well plates (cellstar, cat#: 662 160) coated with poly-D-lysine (0.1 mg/ml, gibco, ref#: A38904-01) in the concentration of 6000 cells/cm^2. The cells were stored in the incubator at 37 °C and 5% CO2. An induction medium (DMEM containing 20 mM sterile ascorbic acid (1:100) and 9% Ficoll v/v fractional volume occupancy (FVO) (18.75 mg/ml Ficoll 70(Cytiva) and 12.50 mg/ml Ficoll 400(Cytiva) (39)) was added to all wells on day one and the induction medium was changed every two to three days until day ten (figure 4), where all wells were decellularized as described in the following.

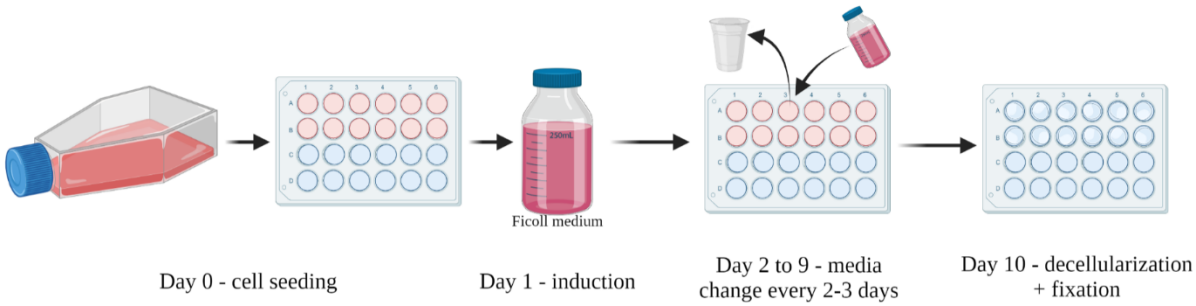

Figure 4 - Illustration of the cultivation period from day zero to day ten. Initially, on day zero, cells were trypsinized from the T75 flask and counted before cells were seeded in 24-well plates. On day one the cells were induced by removing and replacing culture medium with induction medium (DMEM containing Ficoll 70 and -400 (1:6), and 20mM ascorbic acid (1:100)). The Induction medium was replaced every two to three days until day ten when the plates were decellularized.

2.1.3 Decellularization and fixation

The Ficoll-medium was removed from all wells, and they were rinsed with prewarmed (37°C) PBS. An extraction buffer (EB) prewarmed to 37°C consisting of 1% Triton X-100 and 20mM ammonium hydroxide (NH4OH) in PBS was added to all wells and incubated for five min at 37°C. After incubation, PBS was added to the wells in a 1:1 ratio with the EB. The EB and PBS solution was then removed and an additional wash with PBS was carried out on a horizontal shaker (HS 501, IKA) for 20 min. PBS was removed and fixative was added, depending on the analysis to be performed after this step (figure 5).

The samples for collagen concentration were fixed with Kahle fixative (26.6% ethanol, 3.7% formaldehyde, and 2% glacial acetic acid in milli-Q water) and the samples for the indirect immunofluorescence staining of ECM-proteins were fixed with 4% formalin. The samples fixed with Kahle, and the samples fixed with formalin were incubated at RT for ten mins before the fixate was replaced with PBS and the plates were wrapped in parafilm and stored at 4°C.

To assess the content of glycosaminoglycans in the ECM from both fibroblasts and ASCs a solution of papain extraction reagent (0.005% papain crystallized suspension (Sigma-Aldrich (P3125)) in 0.2 M phosphate buffer, pH 6.4 containing 0.8% sodium acetate, 0.4% EDTA (disodium salt), 0.08% L-cysteine) was added to all wells and incubated at 65 °C for three hours with occasional mixing. Further processing of the samples is described in 2.1.7.

The ECM scaffolds intended for assessment of macrophage behavior on ECM scaffolds for were during the decellularization incubated with protease-inhibitor (cat#: 78430, Thermo Scientific) in the ratio 1:100 with EB, and no fixative was added to the scaffolds. After the PBS wash on the horizontal shaker, the PBS was removed from all wells and DNase working solution (DNase 1 (100 U/ml) (cat#: 9003-98-9, Sigma), 5 mM MgCl, 130 μM $CaCl_2$ in PBS) was added slowly to each well and incubated at 37 °C for 30 min. The DNase working solution was removed and the wells were carefully washed twice with PBS. The second wash with PBS was left in the wells and the plates were sealed tightly and incubated at 4°C on an orbital shaker overnight. Lastly, the ECM scaffolds were sterilized in a UV crosslinker (Stratalinker 1800, Stratagene) for five mins.

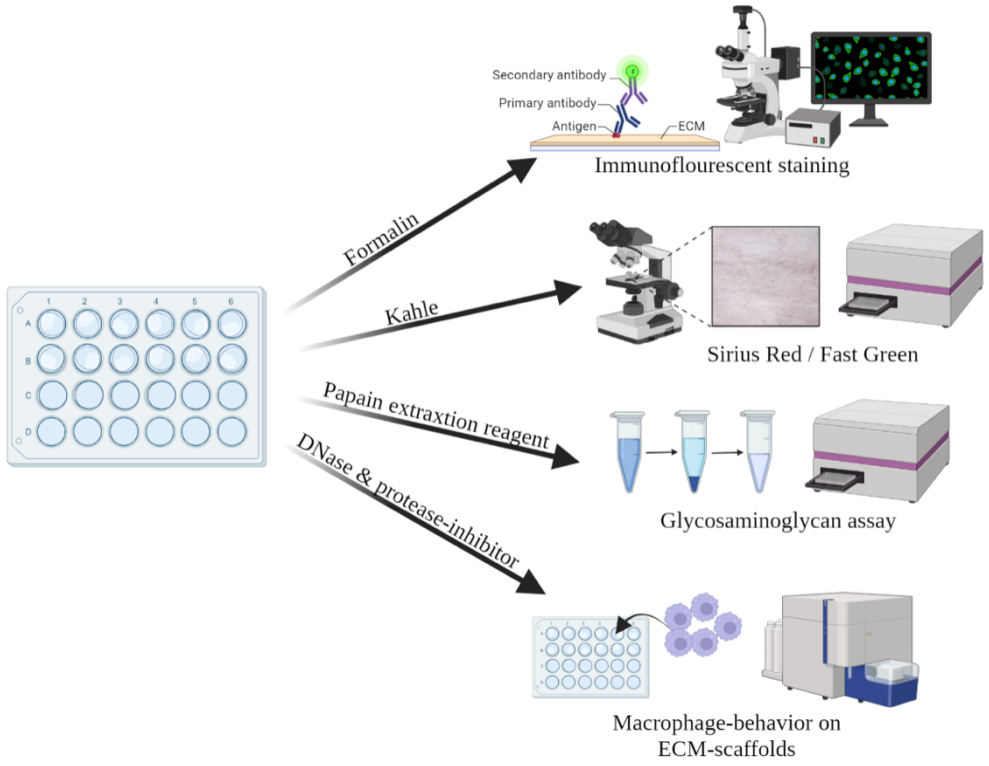

Figure 5 - Overview over the different decellularization and fixation treatments depending on the assessment method.

2.1.4 Assessment of collagen concentration in ECM-scaffolds (Sirius Red/Fast Green (SR/FG))

A Sirius Red/Fast Green (SR/FG) staining kit from Chondrex was used to quantitatively assess the collagen content in the ECM from ASCs and fibroblasts. The preparation before staining has been described in 2.1.3. PBS was removed from all wells with Kahle-fixed ECM and the Sirius Red/Fast Green dye solution was added and incubated for 30 minutes on an orbital shaker (The Belly Dancer®, Stovall Life Science) at RT. After the incubation period, the wells were thoroughly rinsed with distilled water until the water was clear. The stained ECM was photographed using a digital camera (PixeLINK) and the PixeLINK capture OEM software (2004) before dye extraction buffer was added to all wells. The ECM was rinsed with dye extraction buffer until all the dye was eluted. The eluted dye from each well was collected and transferred to a 96-wells plate in triplets, whereafter the optical density (OD) was measured. The OD was measured using the EnSpire Multi-mode Plate Reader (PerkinElmer) at 540 nanometers (nm) (Sirius Red) and 605 nm (Fast Green). According to the manufacturer and as described in the protocol for the staining kit, the collagen concentration can be calculated as described in the following formula:

$$Collagen\ \left(\frac{\mu g}{section}\right) = \frac{OD\ 540\ value - (OD605\ value \cdot 0.291)}{0.0378}$$

Fast Green contributes 29.1% to the OD 540 value. Therefore, subtracting 29.1% of the OD 605 value corrects this contribution and the collagen concentration can then be calculated by dividing the OD 540 value by the color equivalence for collagen (OD values/µg protein) which is 0.0378 OD value/µg protein. The color equivalence for non-collagenous protein is 0.00204 OD value/µg protein, and the concentration of non-collagenous protein can therefore be calculated by dividing the OD 605 value with 0.00204 OD value/µg protein.

2.1.5 Assessment of ECM-related proteins using immunofluorescence

The samples fixated in 4% formalin were assessed using immunofluorescence. The samples were blocked by adding a solution of 1% bovine serum albumin (BSA) in PBS to each well and then incubated for 30 mins at RT. The PBS-BSA solution was replaced with a master mix (panel 1-3) of the antibodies diluted 1:200 in PBS-BSA, as described in table 1, and incubated overnight at 4°C on an orbital shaker.

	Anti-antibody (1:200)	**Host animal**	**Secondary antibody (1:500)**
Panel 1	Collagen I*	Mouse	Alexa Flour 488 (donkey anti-mouse)***
	Collagen III**	Goat	Alexa Flour 350 (donkey anti-goat)***
Panel 2	Laminin*	Mouse	Alexa Flour 488 (donkey anti-mouse)***
	Fibronectin***	Rabbit	Alexa Flour 555 (Goat anti-rabbit)***
Panel 3	Chondroitin sulfate****	Mouse	Alexa Flour 488 (donkey anti-mouse)***

*Table 1 - Overview of antibody panels for immunofluorescent staining. *Sigma-Aldrich, ** Southern Biotech ***Thermo fisher, ****BD Biosciences*

The next day, the samples were washed two times with PBS before incubation at RT for one hour with secondary antibody, diluted 1:500 in PBS-BSA, according to able 1. All samples were photographed with a digital camera (Hamamatsu, ORCA Flash 4.0) under an inverted microscope (AxioObserver.Z1, Carl Zeiss) and using the ZEN 2012 software package (Carl Zeiss).

2.1.6 Assessment of ECM-related genes

Cells were seeded in poly-D-lysine coated 6-well plates (cat#: 657 160, cellstar, greiner bio-one) at a concentration of 6000 cells/cm^2. On day one after seeding the cells, they were induced with induction medium. Cell lysis was performed 24 hours and 36 hours after induction.

2.1.6.1 Cell lysis

The induction medium was removed, and the wells were washed twice with PBS. Total RNA lysis solution (Bio-Rad, cat#: 732-6802) was added to one well at a time and resuspended in the well several times before the solution was transferred to an Eppendorf tube containing 70% ethanol and mixed. The Eppendorf tubes containing the samples were kept on ice before being stored at -80°C.

2.1.6.2 RNA purification and cDNA synthesis

The lysed samples were thawed at RT before the Aurum™ Total RNA Mini Kit from Bio-Rad (cat#: 7326820) was used to perform RNA purification. The samples were transferred to RNA-binding columns in two ml tubes and centrifuged for one min at 12.000 G and 4°C. The filtrate was discarded, and the samples were put through a series of high- and low-stringency washes according to the protocol from the manufacturer. After the last stringency wash, the filtrate was discarded, and the samples were centrifuged for an additional two mins before the RNA-binding columns were transferred to new sterile capped tubes. Elution solution, preheated to 75°C, was then transferred to each column and the samples were centrifuged for two mins whereafter the columns were removed, and the samples were assessed using the nanodrop spectrophotometer (Fisher Scientific, USA). All samples were then normalized to the same concentration of RNA and each sample was transferred to individual sterile tubes containing a 5:1 mix of 5X iSCRIPT reaction mix and iSCRIPT reverse transcriptase. The samples were placed in a thermal cycler (Perkin Elmer) incubated at 25°C for five mins, 42°C for 30 mins, 85°C for five min, and lastly at 4°C before being stored at -20°C.

2.1.6.3 Quantitative polymerase chain reaction (qPCR)

A master mix containing forward primer, reverse primer and SYBR green (BioRad) was prepared for each gene of interest (GOI) (table 2). Samples were prepared by diluting them in RNase-free water (1:100), whereafter samples along with a series of standards and no template control (NTC) were loaded into the 96-well plate in duplicates. An optical plate cover was applied to the plate before it was vortexed and centrifuged at 1200 RPM for five mins. The plate was transferred to the PCR machine where it was run through a PCR protocol with an activation step, a combined denaturation- and annealing step, and

lastly, a melt curve step. The activation step was performed for five mins at 95°C, whereafter 40 cycles of denaturation for 15 sec at 95°C and annealing for 30 sec at 62°C were completed. Lastly, a melt curve was run from 62°C to 95°C.

Gene	Forward primer	Reverse primer	Ta
Peptidylprolyl Isomerase A (*PPIA*)	TCC TGG CAT CTT GTC CAT G	CCA TCC AAC CAC TCA GTC TTG	60 °C
Collagen type 1 alpha 1 (*COL1*)	CCT GGA TGC CAT CAA AGT CT	AAT CCA TCG GTC ATG CTC TC	62 °C
Collagen type 3 alpha 1 (*COL3*)	TAC GGC AAT CCT GAA CTT CC	GTG TGT TTC GTG CAA CCA TC	61 °C
Fibronectin (*FIB*)	ACC TAC GGA TGA CTC GTG CTT TGA CAA AGC	CAA AGC CTA AGC ACT GGC ACA ACA	62 °C
Matrix metalloproteinase 1 (*MMP1*)	TGT GGT GTC TCA CAG CTT CC	CAC TGG GCC ACT ATT TCT CC	62 °C
Matrix metalloproteinase 2 (*MMP2*)	TGC TCG TGC CTT CCA AGT CTG	ATG AGC CAG GAG TCC GTC CTT	62 °C
Tissue inhibitors of metalloproteinases 1 (*TIMP1*)	TTT GTG GCT CCC TGG AAC AGC	ACT GTG CAT TCC TCA CAG CCA A	62 °C
Hyaluronan synthase 2 (*HAS2*)	ACA AAC ATC ACT TGT GGA TGA CC	TA CCC CGG TAG AAG AGC TGG	62 °C

Table 2 - Overview of genes of interest including their primer base sequences and annealing temperature (Ta).

The following pre-validated primers were available at Aalborg University (AAU): peptidylprolyl Isomerase A (*PPIA*), collagen type 1 alpha 1 (*COL1*), collagen type 3 alpha 1 (*COL3*), fibronectin (*FIB*), matrix metalloproteinase 1 (*MMP1*), and hyaluronan synthase 2 (*HAS2*). The primers for matrix metalloproteinase 2 (*MMP2*) and tissue inhibitors of metalloproteinases 1 (*TIMP1*) were designed from the criteria described in appendix 2.

2.1.6.4 Quantification of qPCR-results

The PCR results were quantified using the pfaffl-method where the PCR amplification efficiency was used instead of assuming a 100% PCR amplification efficiency as in the $2^{-\Delta\Delta CT}$ method. The efficiencies for the different GOIs used in the quantification of the PCR results are presented in appendix 3.

2.1.7 Assessment of Glycosaminoglycan (GAG) content in ECM

The glycosaminoglycan (GAG) assay was performed using the Blyscan™ Glycosaminoglycan Assay-kit from biocolor (cat#: B1000, Biocolor). The preparation for the assay is described under 2.1.4. A series of standards containing 0.5, 1, 1.5, 2, 2.5, 3, 4, and 5 µg sulfated GAG (sGAG) was prepared using the Blyscan sGAG reference standard from the kit. After the 3 hours incubation period with papain extraction reagent, the contents of the

wells were thoroughly mixed by pipetting up and down before transferring them to Eppendorf tubes. The tubes were centrifuged at 10,000 G for ten mins, after which the supernatant was transferred to new tubes. Blyscan dye reagent was added to all samples, standards, and blanks before they were placed on a mechanical shaker for 30 mins. The tubes were then centrifuged for ten mins at 13.000 G, and the supernatant was carefully removed. The dye dissociation reagent was added to all tubes, and the tubes were vortexed until all the dye had dissolved. In a flat-bottomed 96-well plate samples, standards, and blanks were loaded in duplicates, and the absorbance was measured at OD 656 nm in a multiplate reader.

The absorbance for the standards was plotted against known sGAG concentrations and the sGAG concentration for each sample was calculated using the formula given by the linear regression in appendix 5.

2.2 Assessment of macrophage behavior on ECM-scaffolds

The monocytes used in this study were isolated from buffy coats donated by healthy donors (Department of Clinical Immunology, Rigshospitalet, Denmark) containing peripheral blood mononuclear cells (PBMCs). CD14+ monocytes were isolated from PBMCs using magnetic-activated cell sorting (MACS) labeled with CD14 beads.

2.2.1 Initiation of CD14+ monocyte cultures

Cryopreserved CD14+ monocytes were thawed in a water bath at 37 °C for five mins. The cells were transferred to a centrifuge tube containing preheated culture medium (RPMI-1640, 10% FBS, 1% penicillin/streptomycin) and centrifuged for five min at 300 G. The supernatant was discarded, and the pellet was resuspended in new culture medium before they were counted on a NucleoCounter NC100 (Chemometec, Denmark), and transferred to an untreated 12-well plate.

2.2.2 Macrophage differentiation

To induce differentiation of the CD14+ monocytes into immature M1(iM1) and –M2 (iM2) macrophages, a polarization medium containing a final concentration of 10 ng/ml granulocyte-macrophage colony-stimulating factor (GM-CSF) (PeproTech) and 75 ng/ml macrophage colony-stimulating factor (M-CSF) (PeproTech) was added to the wells respectively (figure 6). Optimal concentrations of both GM-CSF and M-CSF have previously been

determined by titrations performed by Stine Bangsgaard Hansen from the Cardiology Stem Cell Center at Rigshospitalet, Denmark. The polarization medium was replaced after three days.

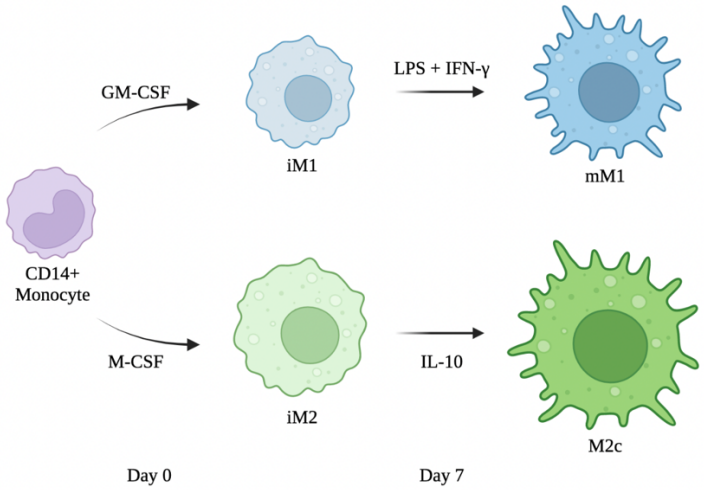

Figure 6 – Differentiation of macrophages. CD14+ monocytes were differentiated to iM1 and iM2 type macrophages by supplementing the medium with GM-CSF and M-CSF, respectively. On day 7 the macrophages were seeded on ECM scaffolds and iM1 was activated with LPS and IFN-g, and iM2 was activated with IL-10 to differentiate into mM1 or M2c, respectively.

2.2.3 Seeding of macrophages on ECM-scaffolds

Seven days after initiation of the CD14+ monocyte cultures and induction of differentiation into iM1 and iM2 macrophages, the iM1 and iM2 macrophages were seeded on ECM scaffolds prepared according to 2.1.4. Initially, culture medium was added to the plates with both ASC- and fibroblast ECM scaffolds and incubated at 37°C. The plates containing the iM1 and iM2 cells were centrifuged at 300 G for five mins before the culture medium was discarded. The cells were washed with PBS and centrifuged as described above, whereafter the supernatant was discarded, and the cells were incubated with TrypLE for 20 mins at 37°C. After the incubation period, the cells were detached and harvested into a tube containing fresh medium and centrifuged for five mins at 300 G. The supernatant was discarded, and the pellet was resuspended in fresh medium before the cell concentration was counted on a NucleoCounter NC100 and normalized to the one with lowest cell concentration. The plates incubated with culture medium were removed from the incubator, and the cells were seeded in the wells containing ECM from both ASCs and Fibroblasts as well as in a 12-well plate without ECM (control).

2.2.4 Activation of iM1 and iM2 macrophages

Differentiation of iM1 macrophages into mature M1 (mM1) macrophages was induced by adding culture medium with a final concentration of 500 ng/ml lipopolysaccharide (LPS) (Sigma-Aldrich) and 5 ng/ml interferon-gamma (IFN-g) (PeproTech) to half of the wells with iM1 macrophages. To induce differentiation of iM2 macrophages into M2c macrophages, medium containing a final concentration of 40 ng/ml IL-10 (PeproTech) was added to half the wells with iM2 macrophages.

2.2.5 Macrophage harvest

On day nine after initiation of monocyte cultures, iM1 and iM2 macrophages, and mM1 and M2c macrophages were harvested for further analysis.

Firstly, the plates were centrifuged at 300 G for five mins, whereafter the supernatant was discarded and replaced with PBS and the plates were incubated for five mins at 37°C. The centrifugation was repeated, and the PBS was replaced with MACS buffer (0.5% FCS and 2 mM EDTA in PBS) and incubated at 4°C for 30 mins. After incubation, the cells were harvested by thoroughly pipetting up and down to ensure detachment of all cells before being transferred to a 15 ml centrifuge tube. An additional wash was carried out with PBS and transferred to the 15 ml tube with cell suspension and then centrifuged at 300 G for five mins. The supernatant was discarded, and the pellet was resuspended in PBS and transferred in duplicates to a 96-well polypropylene plate for further analysis.

2.2.6 Assessment of surface marker expression on macrophages

The 96-well plate with harvested macrophage samples was centrifuged at 300 G for five mins, whereafter the supernatant was discarded. The plate was agitated to dislodge the pellet and PBS was added to all wells. Fixable Viability Stain 780 (FVS780) (cat#: 565388, BD Biosciences) was added at a concentration of ¼ of manufacturer instruct to all wells which were incubated at 4°C for 15 minutes and kept dark. FACS buffer (10% heat-inactivated fetal bovine serum, 1 mM EDTA, and 0.05% sodium azide in PBS) was added to all wells before centrifugation at 300 G for five mins at 4°C. The supernatant was discarded, and the plate agitated to dislodge the pellet. Fc-Block working solution (10 ug/ml human fc-Block in FACS buffer) (cat#: 564219, BD Biosciences) was added to all wells and incubated at four °C for ten mins.

Two Panels of antibody master mix were prepared according to table 3 and added to the wells. Panel 1 was added to one half of the samples and panel 2 was added to the other half of the samples. The plate was incubated for 30 mins at 4°C.

	Antibody (AB)	Dilution	Fluorochrome	Manufacturer
Panel 1	CD1a	1:10	PE	BD Biosciences
	DC-SIGN/CD209	1:20	APC	BD Biosciences
	CD14	1:40	Alexa fluor 488	BD Biosciences
	HLA-DR	1:40	PerCP-Cy5.5	BD Biosciences
Panel 2	CD38	1:40	BB515	BD Biosciences
	ILT-4/CD85d	1:40	APC	Thermo Fisher Scientific
	CD163	1:20	PerCP-Cy5.5	BD Biosciences
	CD206	1:160	PE-Cyamine7	Thermo Fisher Scientific
	CD86	1:320	V450	BD Biosciences

Table 3 3- Overview of antibodies for flowcytometry

Following incubation, FACS buffer was added, and the plate was centrifuged at 4°C for five mins at 300 G, and subsequently, the supernatant was discarded, and the plate was agitated. This step was repeated before the plate was transferred to a fume hood, where cytofix/cytoperm buffer (cat#: 554722, BD Biosciences) was added and resuspended thoroughly in each well before incubation at 4°C for 20 mins. Perm/wash buffer (cat#: 554722, BD Biosciences) was added to each well and the plate was centrifuged at 300 G at 4°C for five mins before the supernatant was discarded, and the plate was agitated. The plate was washed with perm/wash buffer two additional times.

For intracellular staining with CD68 antibody (cat#: 564943, BD Biosciences), the AB was diluted in the ratio 1:40 with perm/wash buffer and added to all wells in panel 1, and perm/wash buffer was added to all wells in panel 2. The plate was incubated for 30 mins at 4°C whereafter it was centrifuged at 4°C and 300 G for 5 mins. The supernatant was discarded before another wash and centrifugation with perm/wash buffer. Lastly, FACS buffer was added to all wells, and the plate was stored at 4°C in darkness overnight. The next day, flow cytometry was performed on a FACSLyric Clinical Flow cytometer (BD Biosciences).

The gating strategy for flow data is illustrated in figure 7. Acquired data were compensated for spill-over between channels by applying a previously established matrix, generated by Stine Bangsgaard Hansen.

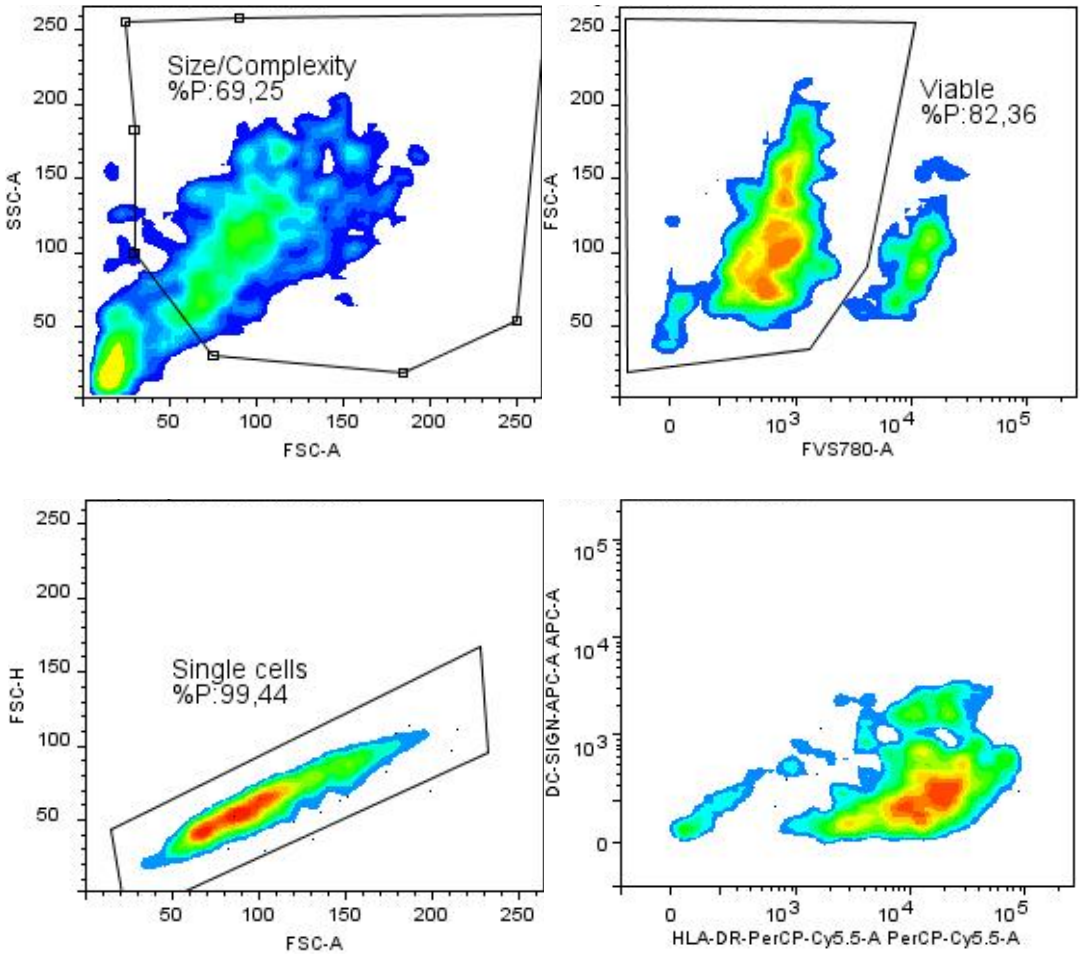

Figure 7 - illustrates the gating strategy used on the flow data. Debris was excluded by gating cell size and complexity. Live cells were gated using side scatter area (FSC-A) vs. FVS780. Then single cells were gated using Forward scatter height (FSC-H) vs forward scatter area (FSC-A). The gating was adjusted to the HLA-DR expression, as this is a known surface marker on iM1 and mM1 macrophages.

2.2.7 Picrosirius red staining

The medium was discarded, and the wells were washed with PBS, and fixed with para-formaldehyde for five to ten mins at RT and washed with PBS. The wells were then washed for five mins with 0.01 M HCL. Picro-Sirius Red (0.1% Sirius (Direct Red 80) in saturated picric acid, Hospital pharmacy Rigshospitalet) was added to each well and incubated at RT overnight protected from light. The next day, the wells were washed for five mins with 0.01 M HCL and then washed with ddH_2O.

Microscopy was performed using an Axio Observer 7 (Zeiss) mounted with a Plan-Apochromat 10x/0.45 Ph1 objective and Axiocam 506 mono camera. The fluorescent properties of Picro-Sirius allow for imaging using filter set 43 (Excitation 545/25 nm, beamsplitter 570 nm, emission 605/70). Exposure times were fixed between acquisitions. The microscopy pictures were processed in Image J, where all pictures were processed the same.

2.3 Statistical analysis

All statistical analysis was performed in IBM SPSS Statistics 27, and acquired data was assumed normally distributed and was therefore analyzed using parametric tests.

The PCR- and flow cytometry data were analyzed using a one-way ANOVA and Bonferroni posthoc correction. Un-paired t-tests were used to analyze the acquired data from the SR/FG and glycosaminoglycan assay. Results where $p<0.05$ were considered significant.

3 Results

3.1 Assessment of extracellular matrix (ECM) deposited by human adipose-derived stem cells (ASCs) and fibroblasts

In the following, the results from the methods used to assess the ECM deposited by ASCs and fibroblasts are presented.

3.1.1 Assessment of collagen concentration in ECM scaffolds (Sirius Red/Fast Green)

The results from the assessment of collagen concentration in the ECM scaffolds are illustrated in figure 8. The staining kit made it possible to visualize the collagenous fibers in the ECM, as Sirius Red binds to those.

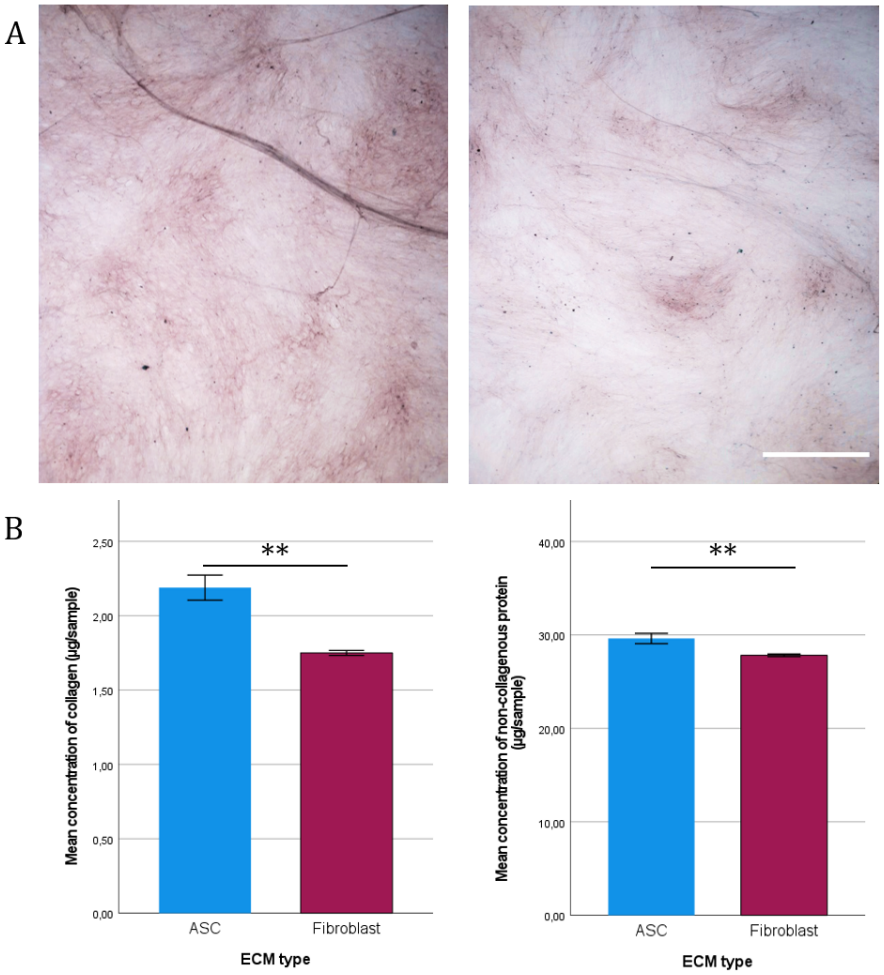

*Figure 8 - A) Sirius Red/Fast green stained images of decellularized ASC ECM and fibroblast ECM. Pictures were taken at a 4x magnification. scalebar: 1000µm. B) The mean concentration of collagenous and non-collagenous protein in the ECM scaffolds derived from ASCs and fibroblasts. The mean collagen concentration pr. sample was for ASC ECM: 2.19 ± 0.08 (SE) µg/sample, and for fibroblast ECM: 1.75 ± 0.02 (SE) µg/sample. The mean concentration of non-collagenous protein pr. sample was 29.63 ± 0.55 (SE) µg/sample for ASC ECM, and 27.83 ± 0.14 (SE) µg/sample for fibroblast ECM. **=p<0.01, n=3.*

A red-stained network of fibers was observed on both the ECM from ASCs and fibroblasts. The network appeared to be denser in the ASC ECM compared to the ECM derived from fibroblasts. The mean collagen concentration for ASC ECM was 2.19 ± 0.08 (SE) µg/sample, and for fibroblast ECM, it was 1.75 ± 0.02 (SE) µg/sample. The mean concentration of non-collagenous protein was 29.63 ± 0.55 (SE) µg/sample for ASC ECM and 27.83 ± 0.14 (SE) µg/sample for fibroblast ECM. Both the concentration of collagen and the concentration of non-collagenous protein were statistically significantly higher in ASC ECM compared to fibroblast ECM.

3.1.2 Assessment of ECM-related proteins using immunofluorescence

Expression of collagen I, collagen III, fibronectin, laminin, and chondroitin sulfate are illustrated in figure 9 A and B.

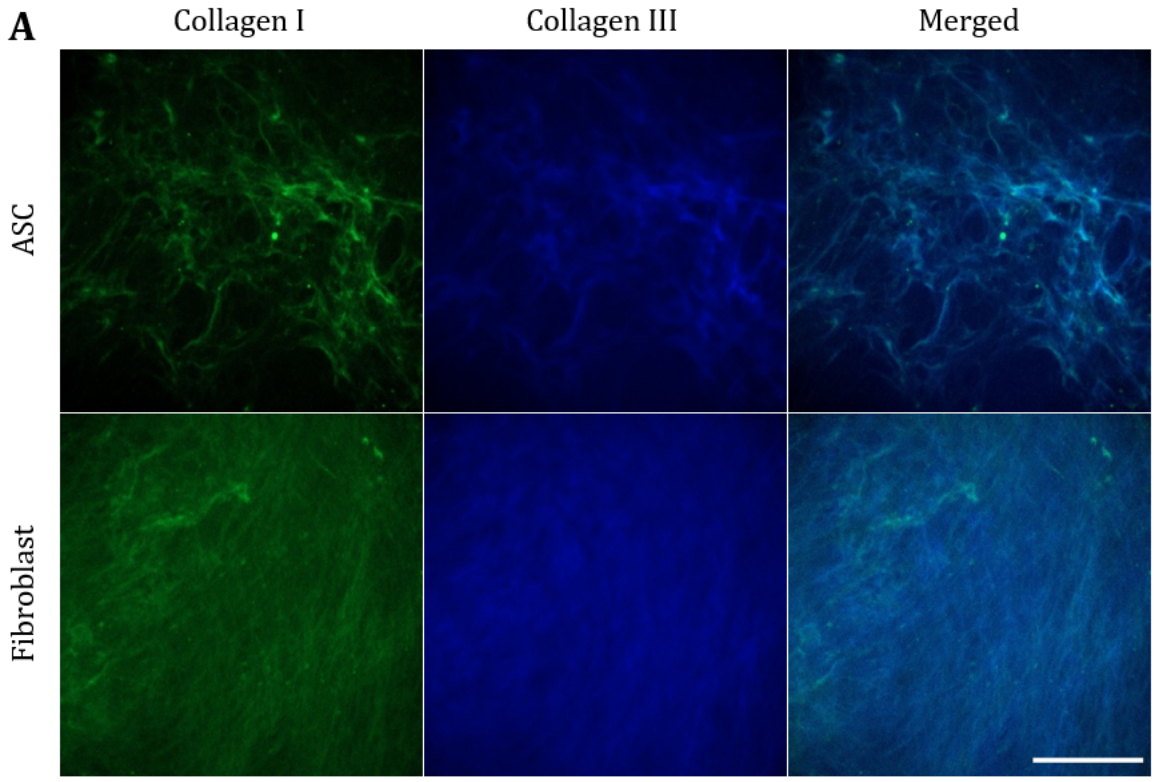

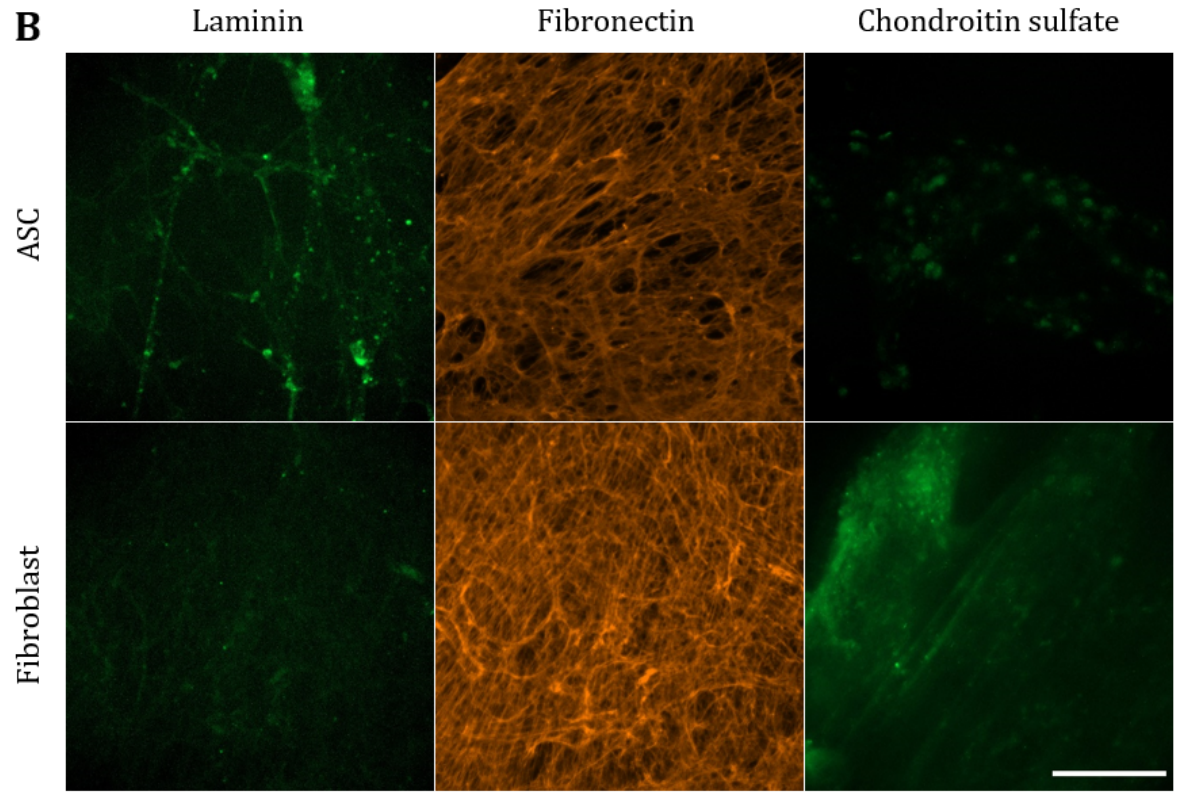

Figure 9 - A) Immunofluorescence images of collagen I and -III in decellularized ASC ECM and fibroblast ECM. B) Laminin, fibronectin, and chondroitin sulfate in decellularized ASC ECM and fibroblast ECM. Scale bar=200 µm

Figure 9A shows immunofluorescence images of collagen type I and III in decellularized ASC- and fibroblast ECM scaffolds. It was observed that the collagen I fibers in the fibroblast ECM were thinner and formed a more parallel and densely packed network than in ASC ECM where the fibers were thicker and more loosely arranged in a web-like structure. The collagen III fibers were not as clearly visualized in the ECM derived from fibroblasts, but, as collagen I, it appears that the collagen III fibers were thicker and more loosely arranged in ASC ECM compared to fibroblast ECM. The composite image shows that collagen III seems to follow the collagen I network.

In figure 9B it is observed that the fibronectin deposited by ASCs, formed a web-like reticular mesh of fibers, and the fibronectin fibers in fibroblast ECM were thin and arranged a denser and more parallel mesh compared to the ASC ECM.

Laminin was present at a low degree in both ASC ECM and fibroblast ECM. The laminin in the ECM produced by ASCs appeared to form a thin network, with occasional accumulations throughout. The laminin in fibroblast ECM is barely detectable, but also seems to form a thin network.

Chondroitin sulfate was barely detectable, especially in ASC ECM (figure 9B). In both types of ECM, the chondroitin sulfate seemed to be present to a low extent at the edges of the ECM scaffold where the ECM is folded.

3.1.3 Assessment of ECM-related genes

The relative gene expression of the genes of interest (GOI) is displayed in figure 10.

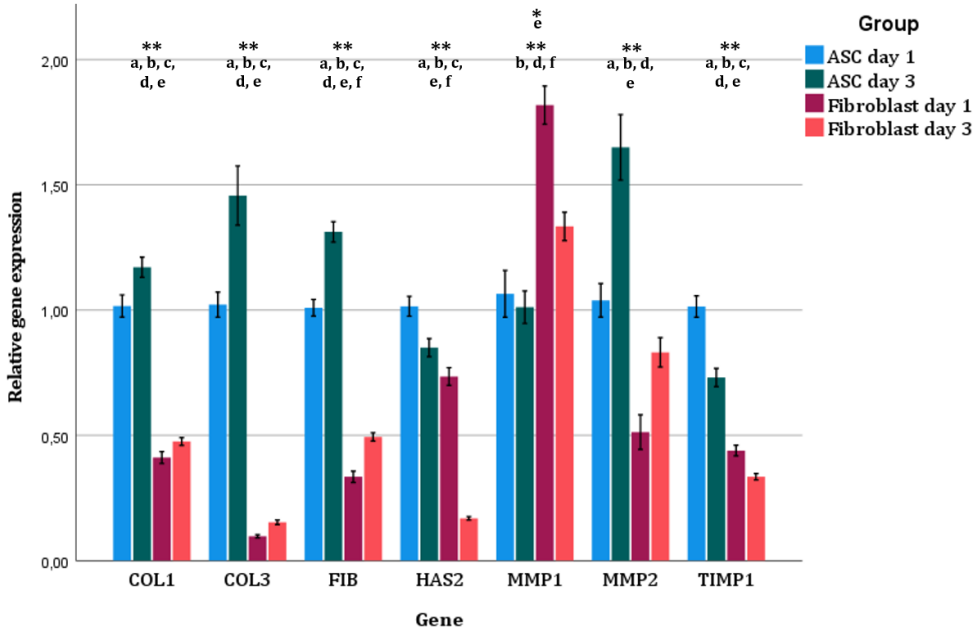

*Figure 10 - Relative gene expression ± 1 SE of the GOI: collagen I (COL1), collagen III (COL3), fibronectin (FIB), hyaluronan synthase 2 (HAS2), matrix metalloproteinase 1 (MMP1), matrix metalloproteinase 2 (MMP2), and tissue inhibitor of metalloproteinases 1 (TIMP1). *=p<0.05, **=p<0.01, a=ASC day 1 vs. ASC day 3, b=ASC day 1 vs. Fibroblast day 1, c=ASC day 1 vs. Fibroblast day 3, d=ASC day 3 vs. Fibroblast day 1, e=ASC day 3 vs. Fibroblast day 3, f=Fibro day 1 vs. Fibroblast day 3. n=9, except for fibroblasts day 1, where n=7.*

The relative gene expression, for both collagen I (*COL1*) and collagen III (*COL3*), consistently increased with time in both groups, although for fibroblasts the difference was not statistically significant. The transcriptional activity of these genes was higher for ASCs at both time points ($p<0.01$). Like *COL1* and *COL3*, the transcriptional activity of fibronectin *(FIB)* was generally higher for ASCs, and the relative gene expression increased with time in both groups ($p<0.01$).

Hyaluronan synthase 2 *(HAS2)*-expression decreased over time in both groups ($p<0.01$). Generally, ASCs had a higher expression of *HAS2*, though no statistically significant difference was found between ASCs on day three compared to fibroblasts on day one ($p>0.05$).

The expression of matrix metalloproteinase 1 *(MMP1)* decreased over time for both ASCs and fibroblasts, however, the decrease was only significant for the fibroblasts. The *MMP1*-expression in fibroblasts was higher compared to ASCs at both time points

(p<0.05). Opposite the expression of *MMP1*, the expression of matrix metalloproteinase 2 *(MMP2)* was higher in ASCs (p<0.01) and increased with time in both groups, however, the increase was only significant for ASCs (p<0.01).

The transcriptional activity for tissue inhibitor of metalloproteinases 1 *(TIMP1)* was higher in ASCs at both time points compared to fibroblasts (p<0.01), and the *TIMP1*-expression decreased over time for both groups, though this was only statistically significant for ASCs (p<0.01)

3.1.4 Assessment of glycosaminoglycan (GAG) content in ECM

As illustrated in figure 11 the mean concentration of sulfated glycosaminoglycans (sGAG)s in decellularized ASC ECM scaffolds was 1.71 ± 0.06 (SE) µg/sample and for decellularized fibroblast ECM scaffolds, the mean sGAG concentration was 3.43 ± 0.04 (SE) µg/sample. The difference in sGAG concentration between decellularized ASC ECM and fibroblast ECM proved to be statistically significant (p<0.01).

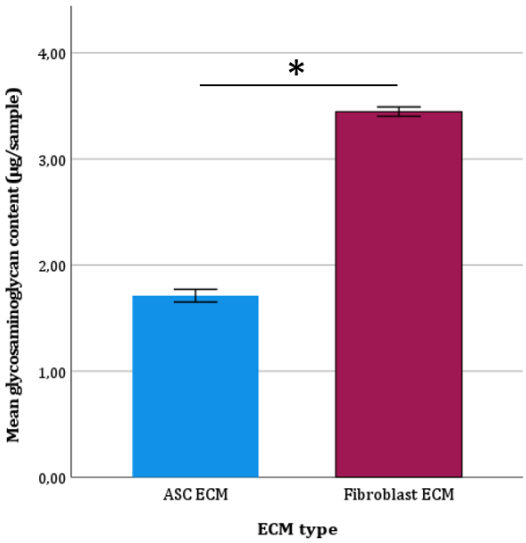

*Figure 11 - The mean concentration of sGAGs in ASCs, 1.71 ± 0.06 (SE) µg/sample, and fibroblasts, 3.43 ± 0.04 (SE) µg/sample. *=p<0.01, n=12*

3.2 Assessment of macrophage behavior on ECM-scaffolds

3.2.1 Macrophage differentiation

The pictures in figure 12 show the differentiation process from CD14+ monocytes to both immature and mature M1 and M2 macrophages. Initially, the monocytes appeared very small and round, whereas they grew larger from day zero to day nine depending on macrophage phenotype. Immature M1(iM1) macrophages appeared smaller than immature

M2(iM2) macrophages on day three, and more iM1 macrophages seemed to be in suspension, whereas a larger amount of iM2 macrophages was flattened out on the bottom of the well. The iM2 macrophages on the bottom of the well were elongated and spindle-shaped and the ones in suspension were rounder. This applied to both the iM1 and iM2 macrophages.

More macrophages, both iM1 and iM2, were situated at the bottom of the well on day seven and compared to day three both iM1 and iM2 macrophages were bigger, while the M2 macrophages still were larger than the iM1 macrophages. Both types of macrophages were round and egg-shaped.

On day nine, some of the mature M1 (mM1) macrophages appeared egg-shaped while others seemed to be more elongated and had protrusions. iM1 macrophages appeared smaller in size and those on the bottom of the well appeared egg-shaped though a lot seemed in suspension. M2c macrophages were large and egg-shaped whereas iM2 macrophages appeared both egg-shaped and shaped like spindles. Both iM2 and M2c macrophages had vacuoles though more appeared to be present in the M2c phenotype.

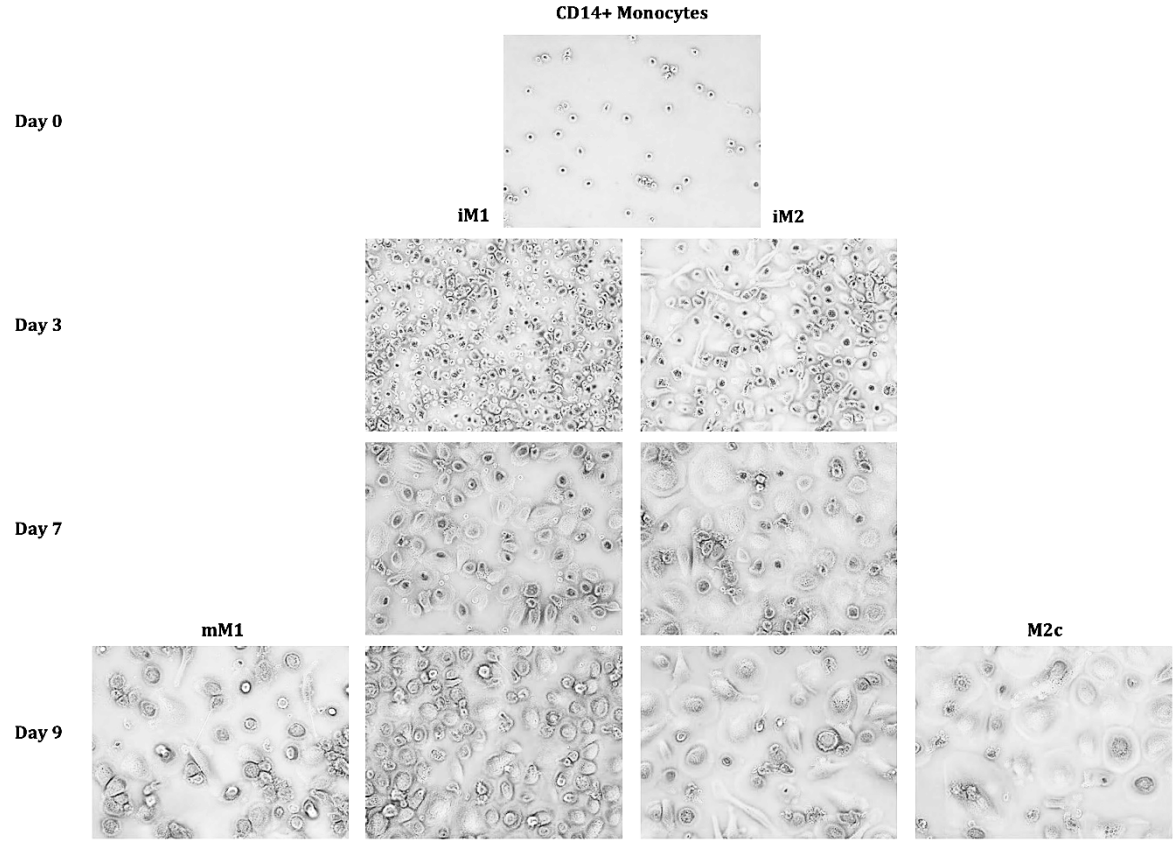

Figure 12 - Illustration of the morphological changes from CD14-positive monocytes on day zero to mature and immature M1 and M2 macrophages on day nine without ECM.

3.2.2 Macrophage differentiation on ASC- and fibroblast-derived ECM scaffolds

The morphology of iM1, iM2, mM1, and M2c macrophages, both in a control plate with no ECM and on ECM scaffolds derived from ASCs and fibroblasts, is shown in figure 13.

On both ASC ECM, fibroblast ECM, and controls the iM1 macrophages were mostly round and egg-shaped. In the control, some of the iM1 macrophages had a more elongated appearance. The iM1 macrophages appeared larger on the fibroblast ECM than in control and ASC ECM. Common to all setups was that most of the macrophages appeared to lie flat on the bottom of the wells and only a few were in suspension.

Applying to all setups, the mM1 macrophages appeared smaller in size compared to iM1 macrophages. The mM1 macrophages appeared oddly shaped and had more rough edges. More mM1 macrophages seemed to be in suspension and only a few macrophages appeared to be at the well bottom in each setup.

The iM2 macrophages across all setups appeared very large compared to both iM1 and mM1 macrophages, and vacuoles were present. The iM2 macrophages on ASC ECM appeared both egg-shaped and elongated whereas most of the iM2 macrophages on fibroblast ECM were egg-shaped and very flat on the well bottom and the edges were difficult to define. The iM2 macrophages in the control plate appeared elongated and some were branching out.

Differences in the morphology of the M2c macrophages were observed between the setups. The M2c control macrophages were very large, round, and elongated. The M2c macrophages on fibroblast ECM appeared to have more cells in suspension than the M2c macrophages on both ASC ECM and control plate and appeared to be generally smaller than the other two setups. The cells on the bottom of the well appeared flat and round or elongated. Some of the M2c macrophages on ASC ECM appeared to have well-defined edges whereas others were more difficult to define. They seemed more oddly shaped and elongated, and very few were egg-shaped. Common to all setups was the high content of vacuoles in the M2c macrophages.

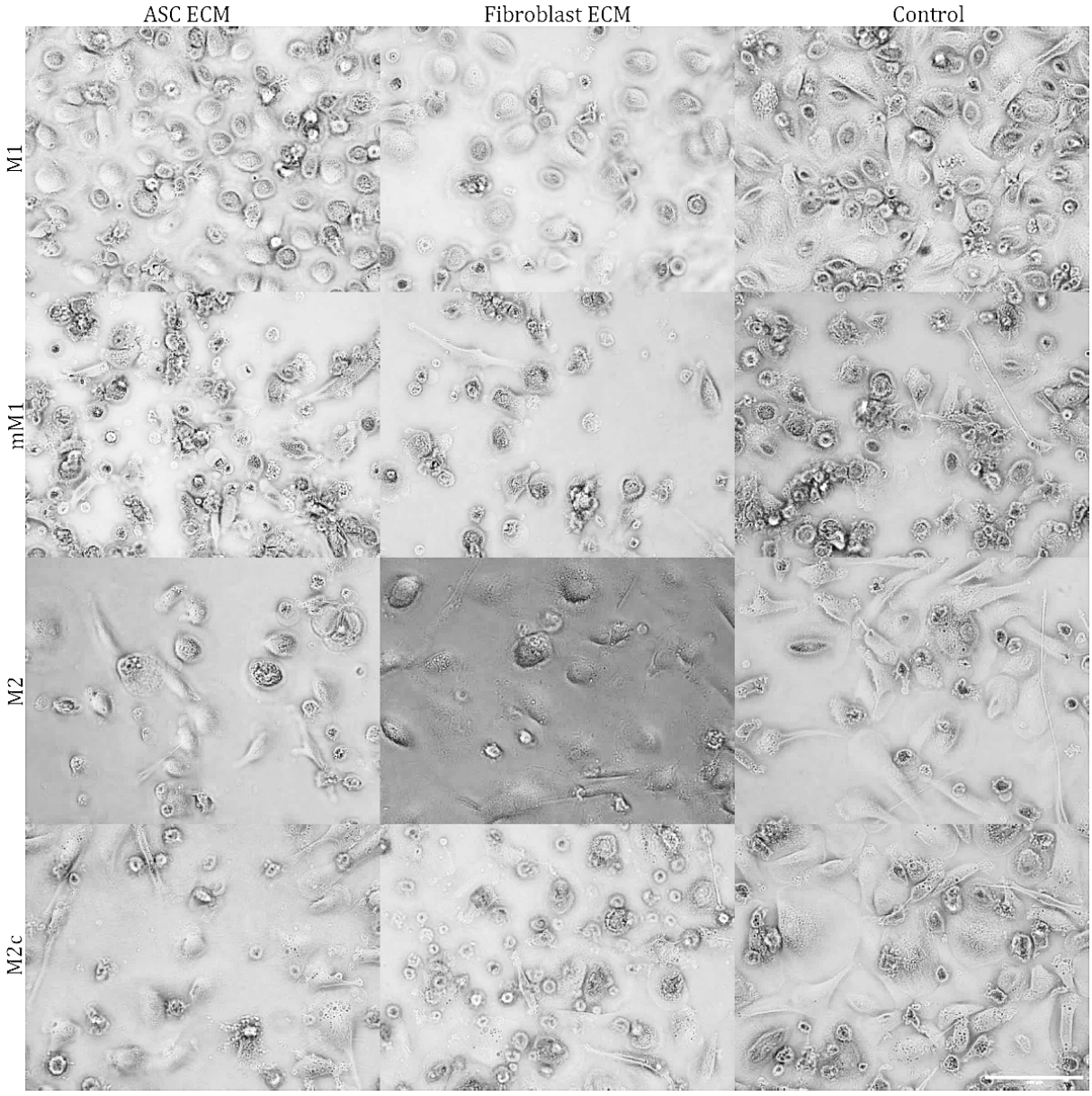

Figure 13 - The morphology of immature M1 and M2 macrophages and mature/activated mM1 and M2c macrophages on both ECM scaffolds derived from ASCs and fibroblasts and control plates without ECM. Scale bar: 100µm

3.2.3 Picrosirius red staining

Figure 14 illustrates images of the processed picrosirius red stained macrophages seeded on ASC ECM, fibroblast ECM, and no ECM (control).

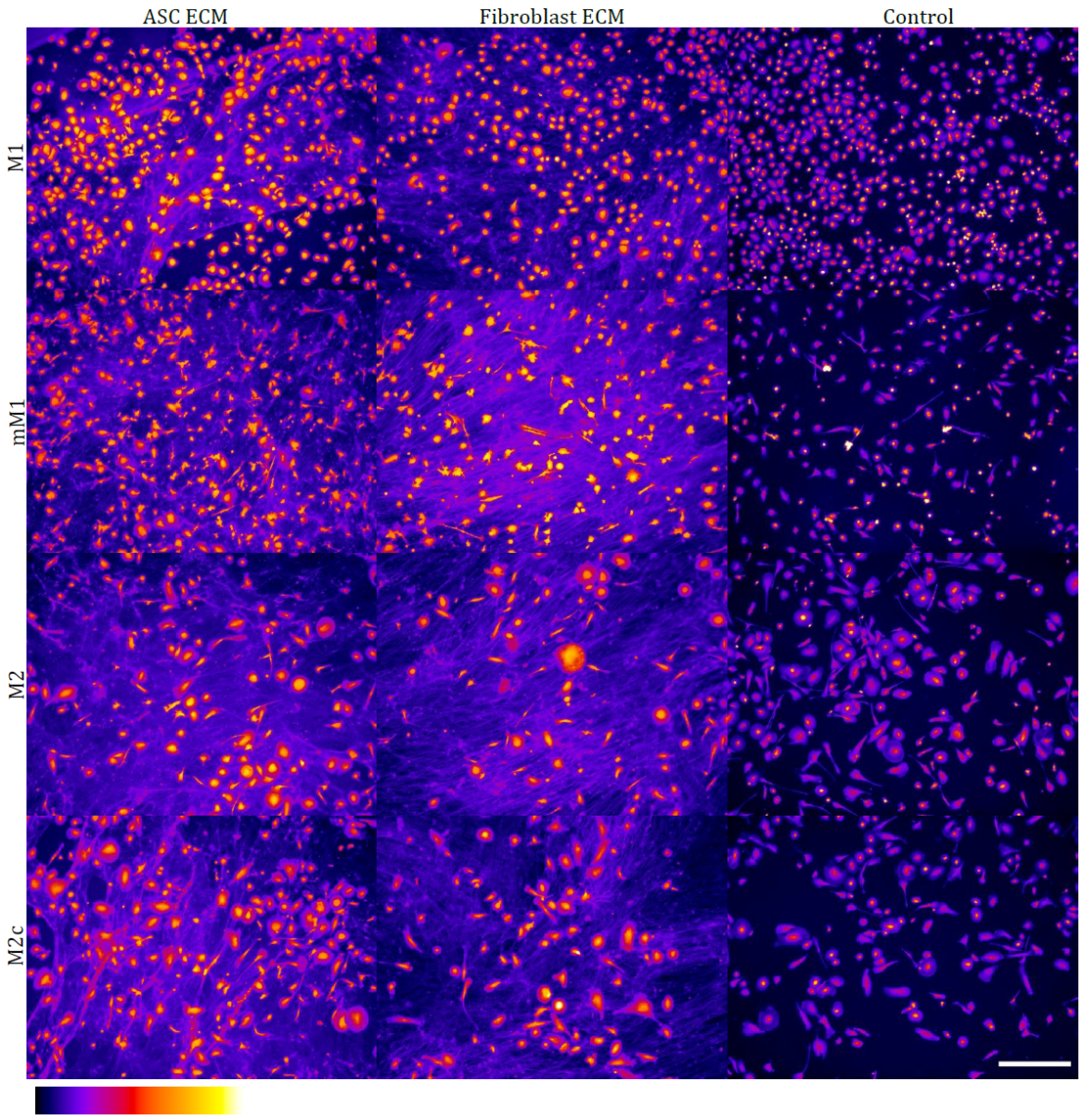

Figure 14 - Overview over picro-sirius stained macrophage phenotypes: M1, M2, mM1, and M2c, on ASC ECM, fibroblast ECM and a control. A LUT (Fire) was used to better visualize the results. In the down left corner of the figure is a scale indicating the colors equivalent to the fluorescent signal. The scale bar measures 300 µm.

The morphological differences and similarities between the different macrophage phenotypes, M1, M2, mM1, and M2c, observed in figure 14 has already been described in 3.2.2. The picrosirius red stain visualized a network of collagen fibers underneath the macrophages. Compared to the controls the macrophages seeded on ECM scaffolds appeared to be elongated along the collagen fibers and seemed to be more branched out, which was more apparent in the mature phenotypes.

3.2.4 Surface marker expression on macrophages

The expression of the markers: CD14, HLA-DR, CD68, CD86, CD206, CD163, CD38, and ILT-4 is presented as the median fluorescent intensity (MFI) on figure 15A and B.

The iM1 macrophages appeared positive for the markers HLA-DR, CD86, CD206, and CD68. The expression of CD206 and CD68 appeared to be higher in iM1 macrophages seeded on ASC ECM compared to those seeded on fibroblast ECM and controls.

The mM1 macrophages appeared positive for the markers HLA-DR, CD68, CD86, CD206, CD38, and ILT-4. The expression of the above-mentioned markers, except CD38, seemed to be higher in mM1 macrophages seeded on ASC ECM compared to the mM1 macrophages seeded in the control plate and on fibroblast ECM. The expression of CD38 seemed to be approximately the same for both mM1 macrophages seeded on ASC ECM and in the control. The HLA-DR, CD38, and CD86 expressions appeared lower on the mM1 seeded on fibroblast ECM compared to both control and ASC ECM.

Both the iM2- and M2c macrophages appeared positive for the markers CD14, CD68, CD163, CD86, and ILT4, the latter seemed to be expressed at a low level. The expression of CD14 appeared higher on M2cs seeded on ASC ECM compared to M2cs seeded on fibroblast ECM, which in turn appeared higher compared to the control. The CD14 expression appeared to be higher on iM2 macrophages on both ASC ECM and in the control, compared to the iM2 macrophages seeded on fibroblast ECM. The CD68 expression seemed to be higher on both iM2 and M2c macrophages seeded on ASC ECM compared to those seeded on the fibroblast ECM and the control. The expression of CD163 seemed to be slightly higher on M2c macrophages in the control, compared to both ECM types, though the expression appeared to be lowest in the M2c macrophages seeded on fibroblast ECM.

All macrophage phenotypes appeared to be negative for both DC-SIGN and CD1a (appendix 6).

Common for all the above-mentioned results were a low number of events, resulting in larger SEs. No statistically significant differences were found between marker expression in the different macrophage phenotypes and ECM-type.

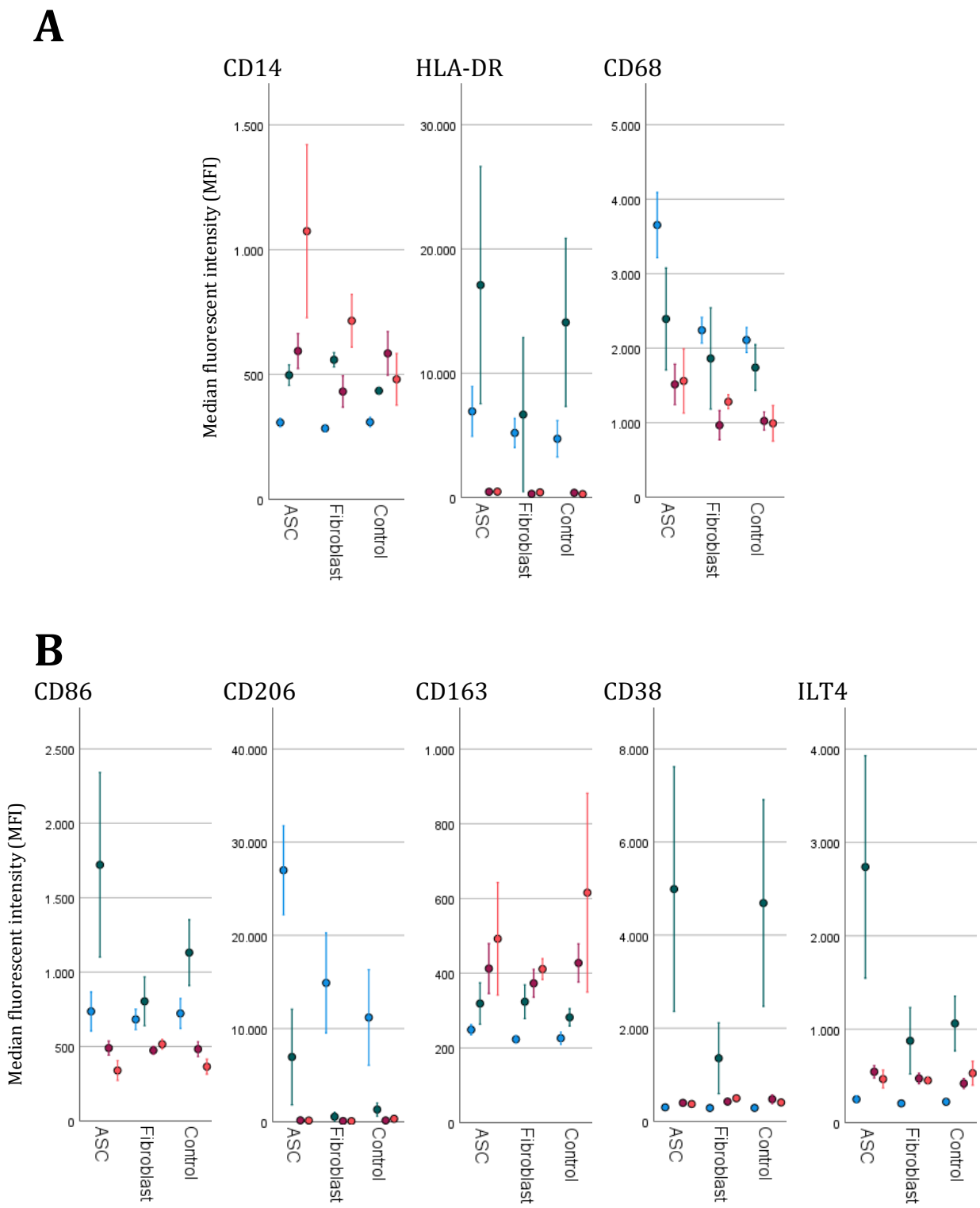

Figure 15 - Graph A illustrates the MFI of the markers CD14, HLA-DR, and CD68 for M1, mM1, M2, and M2c macrophages when seeded on different ECM scaffolds (derived from ASCs vs. derived from fibroblasts) compared to a control. Graph B illustrates the MFI of the markers CD86, CD206, CD163, CD38, and ILT4 for M1, mM1, M2, and M2c macrophages when seeded on different ECM scaffolds (derived from ASCs vs. derived from fibroblasts) compared to a control.

4 Discussion

The properties of the extracellular matrix (ECM) produced by fibroblasts and adipose-derived stem cells (ASCs) and the comparison between them have not been fully elucidated yet. Therefore, the aim of this study was to further clarify some of the key properties of ECM produced by ASC and fibroblasts and to assess the ability of the ECM to modulate macrophage behavior and immunophenotype.

As described in the introduction, collagen I is the most abundant protein in the ECM and collagens are the major structural component of the ECM where they serve as a scaffold for the attachment of cell surface receptors and proteoglycans (40). This study found that the relative gene expression of both collagen I *(COL1)* and collagen III *(COL3)* increased with time for both ASCs and fibroblasts, however, the relative gene expression for both *COL1* and *COL3* was higher in ASCs compared to fibroblasts. This finding is supported by the qualitative Sirius Red/Fast Green (SR/FG) results, where a denser, red-stained network was present in the decellularized ASC ECM scaffolds when compared to the decellularized ECM scaffolds derived from fibroblasts, and the quantitative SR/FG results, which showed a statistically significant higher collagen concentration in the decellularized ASC ECM scaffolds. These findings are consistent with the findings in a study by Paganelli et. al, that investigated the production of collagen I and found that ASCs produced larger amounts of collagen compared to both fibroblasts, and ASC and fibroblast co-cultures. The study by Paganelli et al. also investigated the deposition of collagen from fibroblasts and ASCs using immunofluorescence, where they found that the collagen fiber density was significantly increased in ASC cultures compared to fibroblast cultures (41). This correlates with the immunofluorescent findings in our study, where the collagen fibers appeared thicker in the decellularized ASC ECM compared to the decellularized fibroblast ECM. However, the network of fibers appeared denser and packed tighter in the decellularized fibroblast ECM, contrary to the findings by Paganelli et al. where the ASC ECM cultures had the most abundant collagen deposition (41).

Similar to the results of the collagen concentration assessment, it was found that the gene expression of fibronectin was significantly higher in ASCs compared to the fibroblasts, and this expression increased over time for both cell types. This is also supported by the SR/FG results, where the concentration of non-collagenous protein was significantly higher in ASC ECM compared to fibroblast ECM. However, it is important to note,

that fibronectin is not the only non-collagenous protein in the ECM scaffolds. Contradicting these results are the results obtained from immunofluorescence where fibroblasts seemed to form a slightly denser mesh of fibronectin compared to ASCs. In the study by Paganelli et al., they did not find any noticeable difference in the amount of deposited fibronectin by ASCs versus fibroblasts. Additionally, they discovered that ASCs, supplemented with ascorbic acid, formed a reticular network of fibronectin, while the fibroblasts formed a more parallel pattern of fibronectin (41), which is similar to the findings of our study. However, in our study a denser mesh of fibronectin was generally observed in the ECM produced by fibroblasts, thus suggesting that the amount of fibronectin deposited by fibroblasts is slightly higher than the amount deposited by ASCs. As described earlier, fibronectin is an essential ECM component and has an important role in the organization of ECM and wound healing (42). However, a heavy deposition of fibronectin is seen in hypertrophic scars and keloids, suggesting that the production of too much fibronectin can lead to scar formation (43). Paganelli et al. also described that the parallel pattern of fibronectin is similar to that of scar tissue (41).

The laminin content appeared to be slightly higher in the ASC-derived ECM than in the fibroblast ECM, although the content appeared to be sparse in both types of ECM. Laminin seemed to form a thin network in both groups with small accumulations throughout the network emitting a higher fluorescent signal. This pattern is similar to the deposition of laminin found in a study by Malakpour-Permlid et al. that investigated ECM proteins secreted by fibroblasts cultured in 3D scaffolds (44).

Glycosaminoglycans (GAG)s make up a big part of the proteoglycans which occupy most of the extracellular interstitial space as a hydrated gel (12). An important phase of early wound healing involves the secretion of GAGs by fibroblasts which form a hydrophilic matrix suitable for remodeling during healing (45). Our study showed a statistically significant difference in the content of sulfated GAGs (sGAG)s favoring the decellularized ECM scaffolds derived from fibroblasts where the sGAG content was about double the amount compared to the decellularized ASC ECM scaffolds. The most abundant sGAG, chondroitin sulfate, was also investigated using immunofluorescent staining, where a larger amount of chondroitin sulfate seemed present in the decellularized fibroblast scaffolds, though the amount appeared sparse in both the decellularized ECM scaffolds from ASCs and fibroblasts. This observation agrees with a study by Mahon et al. that also found

little to no sGAG content in decellularized ECMs (46). An important consideration regarding the sGAGs is, however, their configuration. A study by Kosir et al. investigated the characterization of sGAGs synthesized by rat embryo fibroblasts and found that there were two major forms of sGAGs: GAGs connected to the core protein in proteoglycans and free GAG chains. Most of the synthesized GAGs consisted of free chains where chondroitin sulfate was the most abundant and only a small part of chondroitin sulfate is attached to the core proteins of proteoglycans (45). Our concern is that during the decellularization of the ECM scaffold and incubation with both primary-, and secondary antibodies, the samples were subjected to a series of washes possibly resulting in the wash-out of the free GAG chains. This was, however, not investigated further. Though an interesting observation during the imaging process of the immunofluorescent samples was that chondroitin sulfate only appeared to be located on the edges of the ECM scaffolds, where the edges had curled up and maybe caught up some of the free chondroitin sulfate chains.

Hyaluronan (HA) is the GAG responsible for the formation of aggregates contributing to mechanical properties and signaling functions in the ECM by the proteoglycans (18-20). Our study found that ASCs had a higher expression of the hyaluronan synthase 2 *(HAS2)*-gene compared to fibroblasts. However, the transcriptional activity decreased with time in both groups.

Gene expression of *MMP1* decreased over time in fibroblasts; a decrease over time was also observed in ASCs, though this was not significant. A study by Riis et al, also found a decrease in *MMP1* over time, though they only investigated the gene expression in ASCs. Gene expression of *MMP1* was higher in fibroblasts than in ASCs, however, the gene expression of *MMP2* was higher in ASCs than in fibroblasts, and it increased over time. Even if the gene expression of the MMPs is high or low, this may not correspond to the actual activity of the MMPs. As most MMPs are secreted as inactive pro-enzymes, post-translational regulation is an important part of MMP activation. The proMMPs can be allosterically activated through interactions with e.g., different surface molecules and ECM components (47). Though ASCs have a higher *MMP2* gene expression and thus may be capable of synthesizing more MMP2, the MMPs may not be activated, and thus do not execute their function of degrading ECM proteins. The same goes for MMP1 and fibroblasts. Gene expression of *TIMP1* decreased over time but the expression was generally higher in ASCs than in fibroblasts. Because TIMP1 inhibits several MMPs, including MMP1 and MMP2

(48), this may indicate that ASCs have an increased ability to inhibit the degradation of ECM proteins.

The observations regarding the gene expression of ECM proteins suggest that ASCs have an increased turnover of ECM.

In this study, different phenotypes of macrophages were induced from CD14+ monocytes: immature M1(iM1) and -M2(iM2) macrophages, and mature M1 (mM1) and M2c macrophages. Morphological differences were observed between the four phenotypes, however, these were more evident when comparing the M1 phenotypes with the M2 phenotypes, where the M2 phenotypes appeared larger (figure 12 and 13). A difference was also observed in the expression of surface markers, where both iM1 and mM1 macrophages presented as HLA-DR+, CD86+, CD206+, and CD68+, though mM1 were also CD38+ and ILT4+, and both the iM2- and M2c macrophages were CD14+, CD68+, CD163+, CD86+, and ILT4+. iM1 and iM2 macrophages shared some of their surface markers such as CD68 and CD86, however, the difference in other markers allowed discrimination between the two phenotypes. The mM1 macrophages appeared positive for the surface marker CD38, whereas the other phenotypes appeared negative allowing for discrimination of this phenotype. CD38 appeared to be expressed on mM1 macrophages, which is consistent with a study by Amici et al. (34).

Macrophages were seeded on ECM scaffolds derived from ASCs and fibroblasts to investigate the ability of the ECM to modulate macrophage behavior and immunophenotype. Differences in both morphological appearance and surface marker expression were observed between macrophages seeded on ECM scaffolds compared to macrophages without ECM influence.

Morphologically, macrophages seeded on ECM scaffolds appeared different than those in the control group. On the picrosirius red staining, the mM1 and M2c macrophages appeared to have long branches and stretch along the collagen fibers in the ECM scaffold. In a study by Vasse et al., it was observed that collagen affects the macrophage shape, as macrophages seeded on collagen exhibited protrusions and filopodia (49), which is consistent with the findings in our study.

In general, it was observed that the expression of CD14, on M2c, HLA-DR, on iM1 and mM1, CD68, CD86, on mM1, CD206, on iM1 and mM1, and ILT4 on mM1 seemed higher in macrophages seeded on ASC ECM. This suggests that ASC-derived ECM affects surface marker expression differently than fibroblast-derived ECM.

iM2 and the M2c macrophages were found to express little to no CD206, contradicting the literature, describing CD206 as a surface marker for the anti-inflammatory M2 macrophage phenotype (50). Interestingly, CD206 expression appeared to be higher in the iM1 and mM1 macrophages seeded on the ECM scaffolds. This finding is supported by a study by Hulaihel et al. where an increase in CD206 expression was detected on interferon (INF)-γ and lipopolysaccharide (LPS)-activated macrophages seeded with ECM degradation products (51). Another study by Larsen et al. demonstrated that macrophages acquire an immunosuppressive phenotype when cultured in high-density collagen matrices compared to low-density collagen matrices (52). The anti-inflammatory M2 marker CD206 seemed to be expressed at higher levels by macrophages seeded on ASC-derived ECM. This could indicate that the ASC ECM scaffold comprises more collagen than the fibroblast-derived ECM scaffold, which correlates with our results obtained from the SR/FG assessment and the increased *COL1* and *COL3* gene expression in ASCs. These observations suggest a possible immunomodulatory effect of the ASC-derived ECM on the M1 macrophage phenotype.

4.1 Limitations, considerations, and perspectives

An important consideration for future research is the establishment of a protocol applicable and valid for the generation of uniform ECM scaffolds. Even though an optimization was performed on the production of ECM scaffolds in this study (appendix 1), the amount of ECM in the scaffolds was never identical. Sometimes the ECM layer was thicker and denser, and sometimes the ECM appeared thin and fragile. A possible explanation for the variability in produced ECM could be because of the number of cells in the wells. As described under methods, the same number of cells were seeded each time, however, a difference in proliferation rate and confluency was observed varying between setups. This problem was mostly observed with the ASCs.

We encountered issues during the decellularization process, as the ECM scaffolds occasionally detached from the well bottom. Therefore, it is important to be careful when washing the wells containing the ECM scaffold. Additionally, during transportation from Aalborg to Copenhagen the scaffolds also seemed to detach from the wells, resulting in the seeding of macrophages on partially detached and curled up ECM scaffolds.

We discovered that, upon decellularization, the ECM scaffolds in the top or bottom of the plate were more prone to detach. For future knowledge, seeding the cells in the two middle rows is preferable with PBS in the surrounding wells to prevent drying out.

Another limitation of this project was the low event count for the flow cytometry analysis. This unfortunately resulted in big standard errors and made it difficult to conclude anything about surface marker expression. Therefore, the analysis regarding the results of the surface marker expression was based on observed tendencies.

Regarding further research, it would be of interest to assess the cytokine profile of the macrophages seeded on ECM scaffolds.

5 Conclusions

In this study, the ECM deposited by ASCs and fibroblasts in vitro and the ability of the ECM to affect macrophage phenotype and behavior were assessed.

Statistically significant differences were observed in the deposition of ECM components and in the transcriptional activity of ECM-related genes, generally favoring ASCs and ASC ECM, indicating that ASCs had an increased capability to synthesize ECM proteins and an overall increased ECM turnover. These findings indicate that the ECM derived from ASCs is different from the ECM derived from fibroblasts. We found morphological changes in macrophages seeded on ECM scaffolds and that ASC-derived ECM affected the expression of surface markers differently than the fibroblast-derived ECM. Additionally, the results suggest a possible immunomodulatory effect of the ASC-derived ECM on the M1 macrophage phenotype, regarding CD206 expression.

However, further research is necessary to derive a conclusion regarding the differences between fibroblast ECM and ASC ECM and their effects on macrophages.

References

(1) Han G, Ceilley R. Chronic Wound Healing: A Review of Current Management and Treatments. Adv Ther 2017;34(3):599-610.

(2) Porsborg SR. Stamceller og sårheling. Aktuel Naturvidenskab 2021(Nr. 2):34-38.

(3) Verbanic S, Shen Y, Lee J, Deacon JM, Chen IA. Microbial predictors of healing and short-term effect of debridement on the microbiome of chronic wounds. npj Biofilms Microbiomes 2020 -05-01;6(1):1-11.

(4) Velnar T, Bailey T, Smrkolj V. The wound healing process: an overview of the cellular and molecular mechanisms. J Int Med Res 2009 Sep-Oct;37(5):1528-1542.

(5) Riis S, Hansen AC, Johansen L, Lund K, Pedersen C, Pitsa A, et al. Fabrication and characterization of extracellular matrix scaffolds obtained from adipose-derived stem cells. Methods 2020 -01-15;171:68-76.

(6) Krzyszczyk P, Schloss R, Palmer A, Berthiaume F. The Role of Macrophages in Acute and Chronic Wound Healing and Interventions to Promote Pro-wound Healing Phenotypes. Front Physiol 2018 -5-01;9.

(7) Kular JK, Basu S, Sharma RI. The extracellular matrix: Structure, composition, age-related differences, tools for analysis and applications for tissue engineering. J Tissue Eng 2014;5:2041731414557112.

(8) Hyldig K, Riis S, Pennisi CP, Zachar V, Fink T. Implications of Extracellular Matrix Production by Adipose Tissue-Derived Stem Cells for Development of Wound Healing Therapies. Int J Mol Sci 2017 -05-31;18(6).

(9) Ugurlu B, Karaoz E. Comparison of similar cells: Mesenchymal stromal cells and fibroblasts. Acta Histochemica 2020 December 1,;122(8):151634.

(10) Fan C, Liao M, Xie L, Huang L, Lv S, Cai S, et al. Single-Cell Transcriptome Integration Analysis Reveals the Correlation Between Mesenchymal Stromal Cells and Fibroblasts. Frontiers in genetics 2022;13.

(11) Mönch D, Koch J, Dahlke M. Are Mesenchymal Stem Cells Fibroblasts with Benefits? Current Stem Cell Reports 2022;8(2):53-60.

(12) Frantz C, Stewart KM, Weaver VM. The extracellular matrix at a glance. J Cell Sci 2010 -12-15;123(Pt 24):4195-4200.

(13) Murad S, Grove D, Lindberg KA, Reynolds G, Sivarajah A, Pinnell SR. Regulation of collagen synthesis by ascorbic acid. Proc Natl Acad Sci U S A 1981 -05;78(5):2879-2882.

(14) Xue M, Jackson CJ. Extracellular Matrix Reorganization During Wound Healing and Its Impact on Abnormal Scarring. Adv Wound Care (New Rochelle) 2015 -3-01;4(3):119-136.

(15) Hamill KJ, Kligys K, Hopkinson SB, Jones JCR. Laminin deposition in the extracellular matrix: a complex picture
emerges. J Cell Sci 2009 -12-15;122(24):4409-4417.

(16) Schaefer L, Schaefer RM. Proteoglycans: from structural compounds to signaling molecules. Cell Tissue Res 2009 Jun 10,;339(1):237-246.

(17) Li B, Liu H, Zhang Z, Stansfield H, Dordick J, Linhardt R. Analysis of Glycosaminoglycans in Stem Cell Glycomics. Methods in molecular biology (Clifton, N J) 2011 January 1,;690:285-300.

(18) Rogers CJ, Hsieh-Wilson LC. Microarray Method for the Rapid Detection of Glycosaminoglycan–Protein Interactions. Methods Mol Biol 2012;808:321-336.

(19) Wight TN, Toole BP, Hascall VC. Hyaluronan and the Aggregating Proteoglycans. In: Mecham RP, editor. The Extracellular Matrix: an Overview Berlin, Heidelberg: Springer Berlin Heidelberg; 2011. p. 147-195.

(20) Dicker KT, Gurski LA, Pradhan-Bhatt S, Witt RL, Farach-Carson MC, Jia X. Hyaluronan: A Simple Polysaccharide with Diverse Biological Functions. Acta Biomater 2014 -4;10(4):1558-1570.

(21) Fernandes, Célio Jr da Costa, Zambuzzi WF. Fibroblast-secreted trophic factors contribute with ECM remodeling stimulus and upmodulate osteocyte gene markers in osteoblasts. Biochimie 2020 January 1,;168:92-99.

(22) Bonnans C, Chou J, Werb Z. Remodelling the extracellular matrix in development and disease. Nat Rev Mol Cell Biol 2014 -12;15(12):786-801.

(23) Hassanshahi A, Hassanshahi M, Khabbazi S, Hosseini-Khah Z, Peymanfar Y, Ghalamkari S, et al. Adipose-derived stem cells for wound healing. Journal of Cellular Physiology 2019 June 1,;234(6):7903-7914.

(24) Cox TR, Erler JT. Remodeling and homeostasis of the extracellular matrix: implications for fibrotic diseases and cancer. Disease Models & Mechanisms 2011 Mar;4(2):165-178.

(25) Wang P, Huang B, Horng H, Yeh C, Chen Y. Wound healing. Journal of the Chinese Medical Association 2018 February 1,;81(2):94-101.

(26) Guo S, DiPietro LA. Factors Affecting Wound Healing. J Dent Res 2010 -3;89(3):219-229.

(27) Boniakowski AE, Kimball AS, Jacobs BN, Kunkel SL, Gallagher KA. Macrophage-Mediated Inflammation in Normal and Diabetic Wound Healing. The Journal of immunology (1950) 2017 Jul 01,;199(1):17-24.

(28) Bainbridge P. Wound healing and the role of fibroblasts. J Wound Care 2013 -08;22(8):407-412.

(29) Sorg H, Tilkorn DJ, Hager S, Hauser J, Mirastschijski U. Skin Wound Healing: An Update on the Current Knowledge and Concepts. ESR 2017;58(1-2):81-94.

(30) Etich J, Koch M, Wagener R, Zaucke F, Fabri M, Brachvogel B. Gene Expression Profiling of the Extracellular Matrix Signature in Macrophages of Different Activation Status: Relevance for Skin Wound Healing. Int J Mol Sci 2019 -10-14;20(20).

(31) Lucas T, Waisman A, Ranjan R, Roes J, Krieg T, Müller W, et al. Differential roles of macrophages in diverse phases of skin repair. J Immunol 2010 -04-01;184(7):3964-3977.

(32) Yao Y, Xu X, Jin L. Macrophage Polarization in Physiological and Pathological Pregnancy. Frontiers in immunology 2019;10:792.

(33) Orekhov AN, Orekhova VA, Nikiforov NG, Myasoedova VA, Grechko AV, Romanenko EB, et al. Monocyte differentiation and macrophage polarization. Vessel Plus 2019 Mar 21,;2019.

(34) Amici SA, Young NA, Narvaez-Miranda J, Jablonski KA, Arcos J, Rosas L, et al. CD38 Is Robustly Induced in Human Macrophages and Monocytes in Inflammatory Conditions. Front Immunol 2018 -7-10;9.

(35) Hammerbeck C, Goetz C, Newman K, Bonnevier J, Aggeler B. rnd-systems-phenotypic-characterization-human-m1-m2a.

(36) Lam JH, Ng HHM, Lim CJ, Sim XN, Malavasi F, Li H, et al. Expression of CD38 on Macrophages Predicts Improved Prognosis in Hepatocellular Carcinoma. Front Immunol 2019 -9-04;10.

(37) Huang X, Li Y, Fu M, Xin H. Polarizing Macrophages In Vitro. Macrophages 2018 May 15,;1784:119-126.

(38) Sapudom J, Karaman S, Mohamed WKE, Garcia-Sabaté A, Quartey BC, Teo JCM. 3D in vitro M2 macrophage model to mimic modulation of tissue repair. npj Regen Med 2021 -11-30;6(1):1-13.

(39) Fan C, Lim LKP, Loh SQ, Ying Lim KY, Upton Z, Leavesley D. Application of “macromolecular crowding” in vitro to investigate the naphthoquinones shikonin, naphthazarin and related analogues for the treatment of dermal scars. Chemico-Biological Interactions 2019 September 1,;310:108747.

(40) Khoshnoodi J, Cartailler J, Alvares K, Veis A, Hudson BG. Molecular Recognition in the Assembly of Collagens: Terminal Noncollagenous Domains Are Key Recognition Modules in the Formation of Triple Helical Protomers. The Journal of biological chemistry 2006 Dec 15,;281(50):38117-38121.

(41) Paganelli A, Benassi L, Rossi E, Magnoni C. Extracellular matrix deposition by adipose-derived stem cells and fibroblasts: a comparative study. Arch Dermatol Res 2020 -05;312(4):295-299.

(42) Maquart FX, Monboisse JC. Extracellular matrix and wound healing. Pathol Biol (Paris) 2014 -04;62(2):91-95.

(43) Ward Kischer C, Hendrix MJC. Fibronectin (FN) in hypertrophic scars and keloids. Cell Tissue Res 1983;231(1):29-37.

(44) Malakpour-Permlid A, Buzzi I, Hegardt C, Johansson F, Oredsson S. Identification of extracellular matrix proteins secreted by human dermal fibroblasts cultured in 3D electrospun scaffolds. Sci Rep 2021 -03-23;11(1):1-18.

(45) Kosir MA, Quinn CCV, Wang W, Tromp G. Matrix Glycosaminoglycans in the Growth Phase of Fibroblasts: More of the Story in Wound Healing. Journal of Surgical Research 2000 /07/01;92(1):45-52.

(46) Mahon OR, Browe DC, Diaz-Payno PJ, Pitacco P, Cunningham KT, Mills KHG, et al. Extracellular matrix scaffolds derived from different musculoskeletal tissues drive distinct macrophage phenotypes and direct tissue-specific cellular differentiation. Journal of Immunology and Regenerative Medicine 2021 May 1,;12:100041.

(47) Madzharova E, Kastl P, Sabino F, auf dem Keller U. Post-Translational Modification-Dependent Activity of Matrix Metalloproteinases. Int J Mol Sci 2019 -6-24;20(12).

(48) Cabral-Pacheco GA, Garza-Veloz I, Castruita-De la Rosa C, Ramirez-Acuña JM, Perez-Romero BA, Guerrero-Rodriguez JF, et al. The Roles of Matrix Metalloproteinases and Their Inhibitors in Human Diseases. Int J Mol Sci 2020 -12-20;21(24).

(49) Vasse GF, Kühn PT, Zhou Q, Bhusari SA, Reker-Smit C, Melgert BN, et al. Collagen morphology influences macrophage shape and marker expression in vitro. Journal of Immunology and Regenerative Medicine 2018 March 1,;1:13-20.

(50) Suzuki Y, Shirai M, Asada K, Yasui H, Karayama M, Hozumi H, et al. Macrophage mannose receptor, CD206, predict prognosis in patients with pulmonary tuberculosis. Sci Rep 2018 -09-03;8(1):1-9.

(51) Huleihel L, Dziki JL, Bartolacci JG, Rausch T, Scarritt ME, Cramer MC, et al. Macrophage phenotype in response to ECM bioscaffolds. Semin Immunol 2017 -2;29:2-13.

(52) Larsen AMH, Kuczek DE, Kalvisa A, Siersbæk MS, Thorseth M, Johansen AZ, et al. Collagen Density Modulates the Immunosuppressive Functions of Macrophages. J Immunol 2020 -09-01;205(5):1461-1472.

Appendices

A1. Optimizations

Optimizations were performed for the protocol for induction of extracellular matrix (ECM) deposition and decellularization as many issues were observed. Some of these issues are described in the limitations and considerations in the discussion section. It was observed that especially ECM from the adipose-derived stem cells (ASCs) was problematic to work with.

The optimizations performed included the number of cells seeded on day zero of the protocol:
Both ASCs and fibroblasts were seeded in sterile 24-well plates (cellstar, cat#: 662 160) coated with poly-D-lysine (0.1 mg/ml, gibco, ref#: A38904-01) in four different cell concentrations: 3000, 6000, 8000 and 10000 cells/cm^2. The cells were stored in the incubator at 37 °C and 5% CO2. All wells were induced with an induction medium on day one and the induction medium was changed every two to three days until day ten, where all wells were decellularized (described under 2.1.3 Decellularization and fixation) and the collagen concentration in the ECM derived from both ASCs and fibroblasts was analyzed using the Sirius Red / Fast Green staining kit from Chondrex (described under 2.1.4 Assessment of collagen concentration in ECM-scaffolds (Sirius Red/Fast Green). Figure A1 shows the results from the optimization:

A

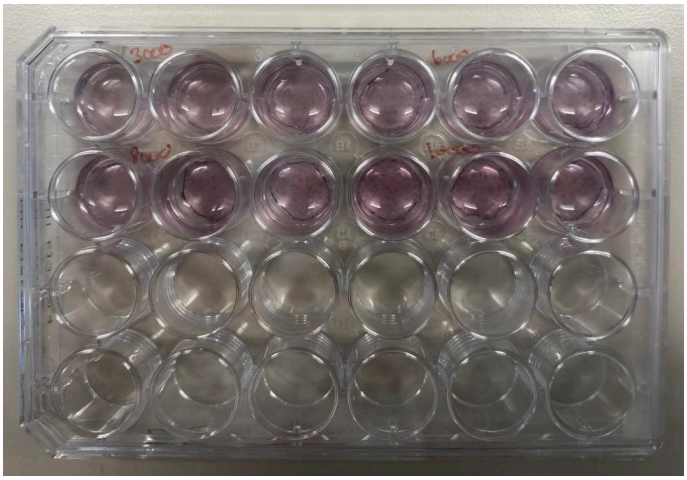

B

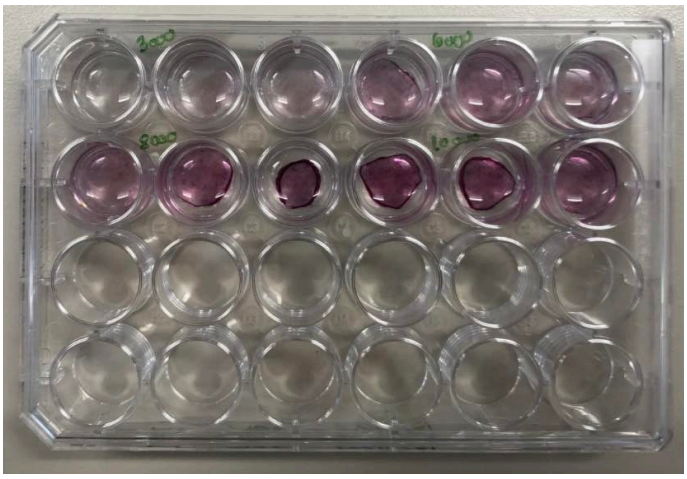

C

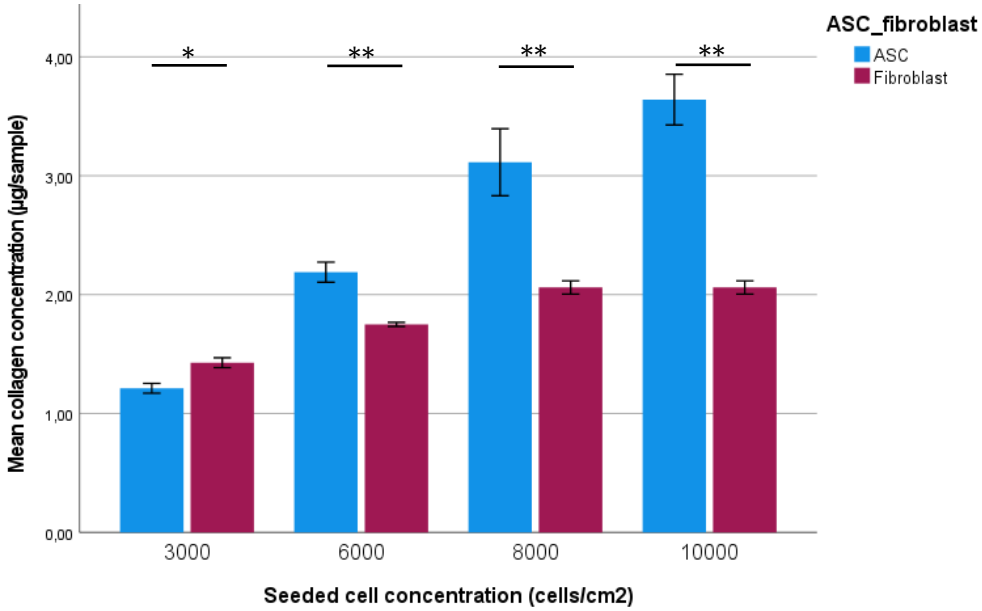

*Figure A16 - A: Picture of the SR/FG-stained ECM scaffolds from fibroblasts in the cell seeding concentrations of 3000, 6000, 8000, and 10.000 cells/cm². B: Picture of the SR/FG-stained ECM scaffolds from ASCs in the cell seeding concentrations of 3000, 6000, 8000, and 10.000 cells/cm². C: Showing the collagen concentration for cell seeding concentrations of 3000, 6000, 8000, and 10.000 cells/cm2. 3000 cells/cm2 = ASC ECM: 1.21 ± 0.12 µg/sample, fibroblast ECM: 1.43 ± 0.12 µg/sample. 6000 cells/cm2 = ASC ECM: 2.19 ± 0.25 µg/sample, fibroblast ECM: 1.75 ± 0.05 µg/sample. 8000 cells/cm2 = ASC ECM: 3.11 ± 0.85 µg/sample, fibroblast ECM: 1.94 ± 0.24 µg/sample. 10.000 cells/cm2 = ASC ECM: 3.64 ± 0.64 µg/sample, fibroblast ECM: 2.06 ± 0.93 µg/sample. *=p<0.05, **=p<0.01. Error bars = ±1 standard error (SE)*

The collagen concentration for the ASC ECM where cells were seeded at a concentration of 3000 cells/cm^2 was 1.21 ± 0.12 (SE) µg/sample, and for fibroblast ECM it was 1.43 ± 0.12 (SE) µg/sample. For ECM where cells were seeded at 6000 cells/cm2, the collagen concentration was 2.19 ± 0.25 (SE) µg/sample for ASC ECM, and 1.75 ± 0.05 (SE) µg/sample for fibroblast ECM. For 8000 cells/cm2 ASC ECM had a collagen concentration of 3.11 ± 0.85 (SE) µg/sample, and for fibroblast ECM it was 1.94 ± 0.24 (SE) µg/sample. The collagen concentration for ECM from the cell seeding concentration of 10.000 cells/cm2 was for ASC ECM 3.64 ± 0.64 (SE) µg/sample, and for fibroblast ECM it was 2.06 ± 0.93 (SE) µg/sample.

Even though the concentration of collagen was higher in the ECM scaffolds, where the cell seeding concentration was 8000 and 10.000 cells/cm^2, other problems were present. As seen in figure 1B, the wells containing ASC ECM where the cell seeding concentration was 8000 and 10.000 cells/cm^2 contained a darker stained ECM. However, the edges were curled up, and the ECM was loose on the well surface. This made the scaffold difficult to use further on in the project, and therefore the best cell seeding density was determined to be 6000 cells/cm^2.

Trouble shooting:

- To help prohibit the ECM from curling up under the decellularization process, use preheated PBS before decellularizing.
- If curled up ECM is observed in the outer wells in the plate à try placing the cells/samples in the middle of the plate and fill the surrounding wells with PBS to prevent the cells from drying out.
- Let the ASCs acclimate to the DMEM for at least a week before seeding them into plates.
- Be aware of the passage number for the ASCs → we observed more problems the higher the passage number.
- Do not let the stem cells get over confluent. It was experienced, that this slowed down their proliferation speed afterwards.

A2. Primer design

The primers designed for this study were designed using Primer-BLAST from NIH. They were designed from the following criteria:

Criteria:	**Value:**
Product size	70-150 base pairs (bp)
Primer length	20
Primer melting temp (tm)	Min: 62, opt: 63, max: 65 Max Tm difference: 1
Primer specificity stringency	At least 4 total mismatches to unintended targets, including 2 mismatches within the last 4 bp at the 3' end.
Primer size	Min: 18, opt:20, max:25
Primer GC content (%)	40-60
Max poly-x	3
Max GC in primer 3' end	3
Self-complementarity	<6
Separated by:	Intron, yes, if no results → exon-exon span

Secondary structures were investigated using the mFOLD online DNA Folding Form (http://www.unafold.org/mfold/applications/dna-folding-form.php). The secondary structures were investigated under default settings apart from the following specifications: 50 mM Na^{+}, 1.5 mM Mg^{++}, and a temperature of 60°C. The primer sequences were checked for the probability of hairpins and primer-dimers using Autodimer (https://www-s.nist.gov/dnaAnalysis/primerToolsPage.do).

A3. Table of amplification efficiency of transcripts

The table below illustrates the amplification efficiencies given by CFX Manager Version: 3.1.1517.0823 (BioRad) used together with the PCR machine to present and quantify the PCR results.

The efficiency of each primer is calculated using the series of standards loaded into the plate with samples and blanks for each gene of interest (GOI). From the series of standards, a standard curve is made plotting the measured Ct values against log starting quantity, and thereafter the efficiency is calculated. This is automatically done by the CFX Manager software, and the efficiencies are calculated using the following formula:

$$E = 10^{-1/slope}$$

The slope is the line derived from the standard curve.

This is then converted to % efficiency by using the formula:

$$\%\, efficiency = (e - 1) \cdot 100$$

The efficiencies calculated for the different GOIs are presented in the table below:

PPIA	COL1	COL3	FIB	HAS2	MMP1	MMP2	TIMP1
79.75%	70.34%	100,1%	67,3%	93,76%	66,47%	75,6%	72,06%

A4. Melt curves

The melt curves for each PCR gene. All curves show a single sharp peak, that is indicative of no presence of non-specific amplification or primer dimer formation A few NTCs showed a small peak.

Peptidylprolyl Isomerase A *(PPIA)*:

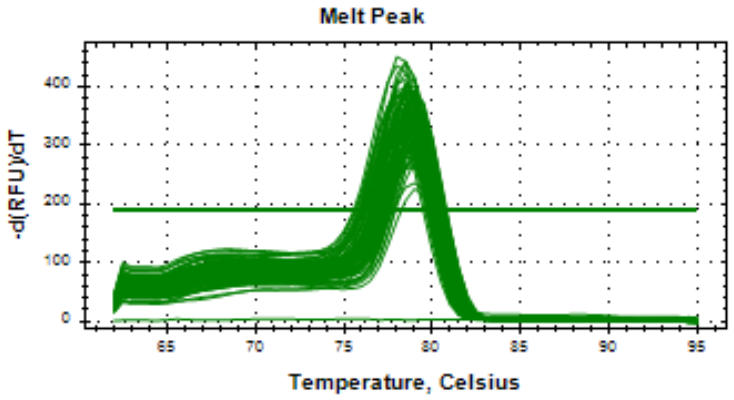

Collagen I *(COL1)*:

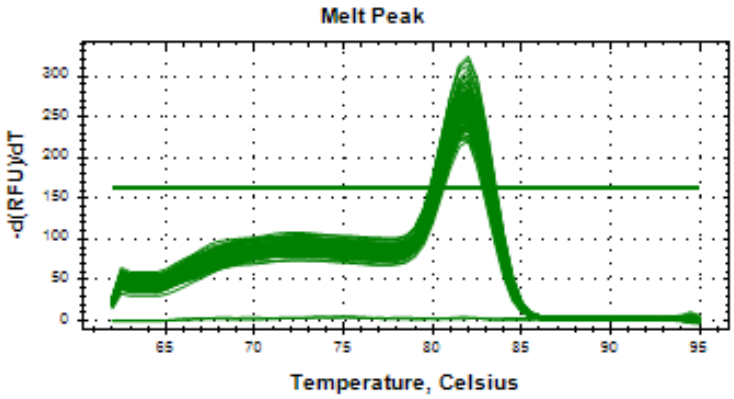

Collagen III *(COL3)*:

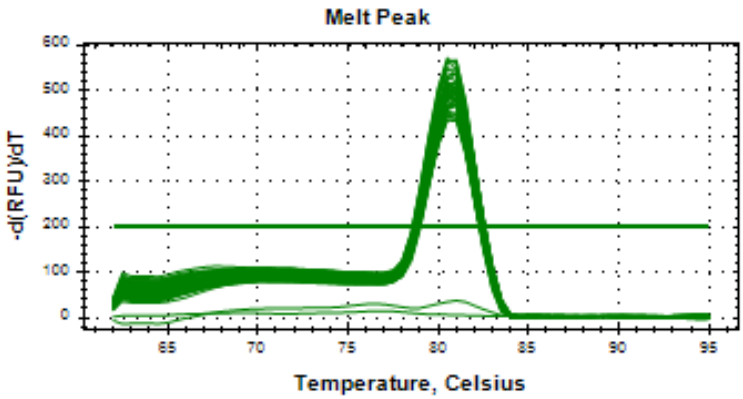

Fibronectin *(FIB)*:

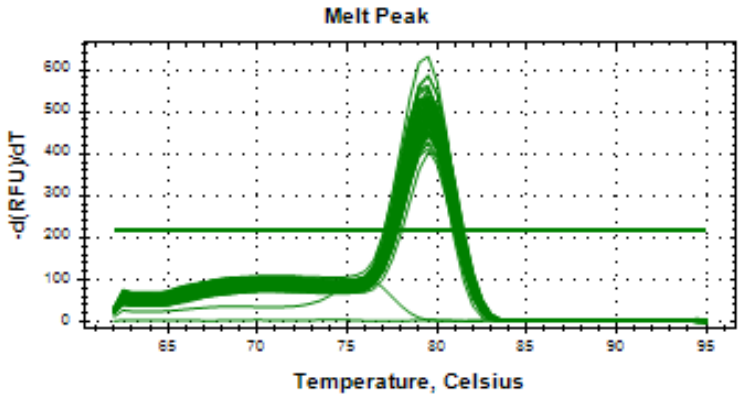

Hyaluronan synthase 2 *(HAS2)*:

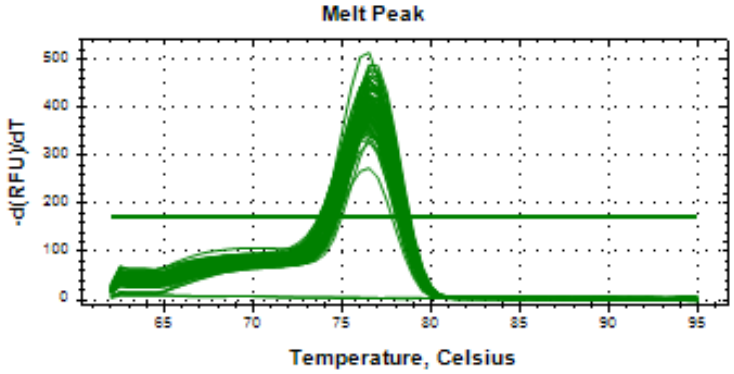

Matrix metalloproteinase 1 *(MMP1)*:

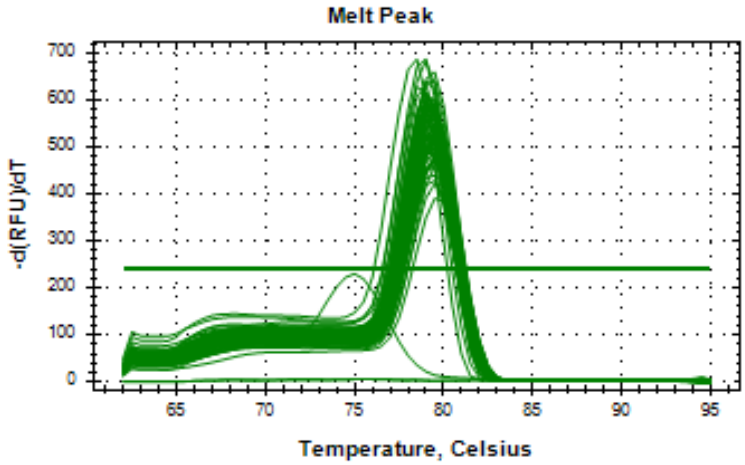

Matrix metalloproteinase 2 *(MMP2)*:

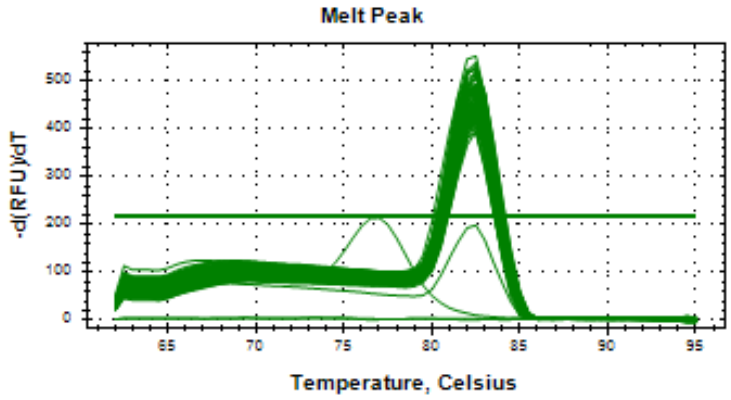

Tissue inhibitor of metalloproteinases 1 *(TIMP1)*:

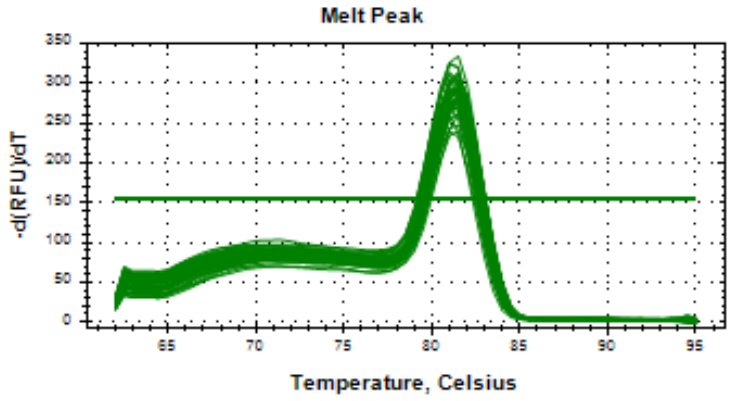

A5. Glycosaminoglycan assay standard curve

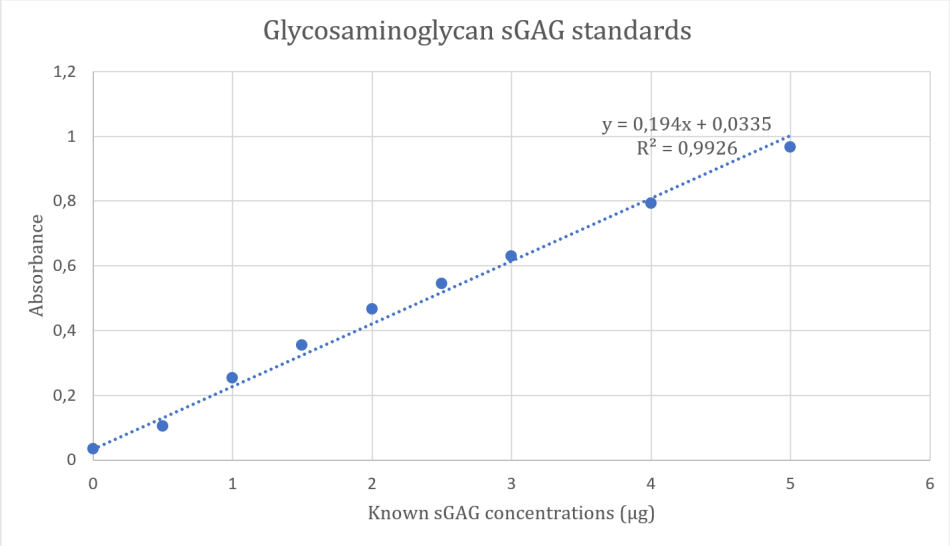

Graph - Standard curve for the standards with known concentration. The OD656-value was plotted against the known concentration of sGAG, and a linear regression was made. R^2=0.9926.

Formula given by the linear regression (also shown in the graph above):

$$y = 0.194x + 0.0335$$

A6. Surface marker expression results for DC-SIGN and CD1a

The graphs illustrate the median fluorescent intensity (MFI) on the y-axis for CD1a and DC-SIGN.

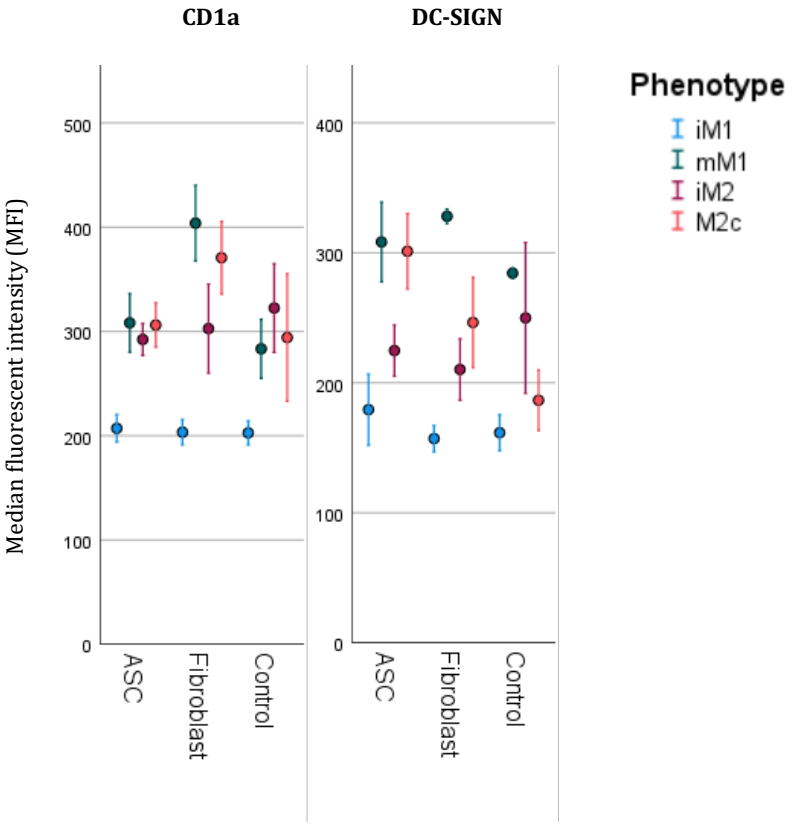

A7. Macrophage ECM culture protocol

Optimized/adjusted protocol for assessment of macrophage behavior on ECM scaffolds.

Medium:

- 500 ml RPMI 1640
- 50 ml FBS (10%)
- 5 ml Pen/Strep

Day 0 (Tuesday, Week 1)

1. Heat up 90 ml medium

Establishing cultures from cryopreserved monocytes

- Retrieve 5 vials of cryopreserved CD14-positive monocytes from liquid nitrogen
    - Locations

Donor	Box	Placement
B	Tank 1, Rack 3, Box 3	4 retrieved
C	Tank 1, Rack 3, Box 3	6G, 7G, 8G, 9G, 10G
D	Tank 1, Rack 3, Box 3	5I, 6I, 7I, 8I, 9I
F	Tank 1, Rack 3, Box 5	6C, 7C, 8C, 9C, 10C

- Place in bag and thaw in water bath (37°C) for 5 minutes
- Transfer to 8 ml preheated medium and centrifuge at 300 g for 5 min (counter-weight: 12 ml)
- Discard of supernatant and resuspend pellet in 6 ml of medium
- Count on nucleocounter:
    - Add 200 µl medium to cell suspension, mix by gentle pipetting, and transfer 200 µl to eppendorf tube.
    - Make a dead count directly on suspension (nucleocassette). Note numbers in table below.
    - Transfer 100 µl cell suspension to new Eppendorf tube. Add 100 µl reagent A and mix. Add 100 reagent B. Count total cell number (nucleocassette)

Donor	Volume	Dead	Total	Dilution factor (DF) 3x	Viable Total * DF - Dead

B	6,2 ml			3	
C	6,2 ml			3	
D	6,2 ml			3	
F	6,2 ml			3	

- Seed 500 µl cell suspension per well in a 12-well plate

Differentiation of macrophage phenotypes

Calculations are per donor. If multiple donors are set up, volumes should be multiplied accordingly.

For **M1 differentiation**, a final concentration of **10 ng/ml GM-CSF** is added. This is generated by addition of a 2x medium (20 ng/ml).

Stock concentration: 50,000 ng/ml. Vial contains 12 µl. Add 48 µl medium to generate 10,000 ng/ml concentration. This formulation is stable for 1-2 days.

We need 3 ml of working solution plus residual waste. Let's say 3.5 ml to play it safe.

$$C1 \times V1 = C2 \times V2 \rightarrow 10{,}000\frac{ng}{ml} \times V1 = 20\frac{ng}{ml} \times 3.5\ ml$$

$$V1 = \frac{20\frac{ng}{ml} \times 3.5\ ml}{10{,}000\frac{ng}{ml}} = 7\ ul$$

☐ Place 3.5 ml medium in a 15 ml tube and add 7 µl GM-CSF. Vortex and add 500 µl per well to respective wells (Figure A1.1).

For 4 donors:

- 1 x cytostock GM-CSF
- Place 14 ml medium in a 15 ml tube and add 28 µl GM-CSF. Vortex and add 500 µl per well to respective wells (Figure A1.1).

For **M2 differentiation**, a final concentration of **75 ng/ml M-CSF** is added. This is generated by addition of a 2x medium (150 ng/ml).
Stock concentration 50,000 ng/ml

- ☐ Add 99 µl fresh medium to stock vial (11µl) to generate a 5,000 ng/ml working solution.

$$C1 \times V1 = C2 \times V2 \rightarrow 5{,}000\frac{ng}{ml} \times V1 = 150\frac{ng}{ml} \times 3.5\ ml$$

$$V1 = \frac{150\frac{ng}{ml} \times 3.5\ ml}{5{,}000\frac{ng}{ml}} = 105\ ul$$

- ☐ Place 3.5 ml medium in a 15 ml tube and add 105 µl M-CSF. Vortex and add 500 µl per well to respective wells (Figure A1.1).

For 4 donors:

- 4 x stock M-CSF (99x4 µl medium + 4x stock (11 µl))
- Place 14 ml medium in a 15 ml tube and add 420 µl M-CSF. Vortex and add 500 µl per well to respective wells (Figure A1.1).

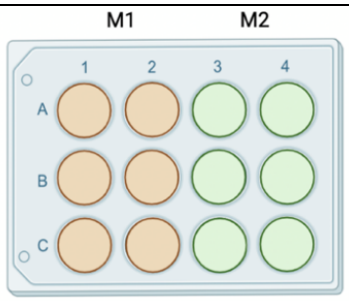

Day 3 (Friday, Week 1)

1. Heat up 52 ml medium

Without removing anything from cultures, add 1 ml medium containing 2x polarizing cytokines (see table below). Volume is now 2 ml/well.

M1	M2
1 ml per well, 6 wells, 4 plates plus waste: 24 + 2 ml Desired concentration: 20 ng/ml GM-CSF Cytostock: Add 48 µl medium to 12 µl stock (50 ug/ml) to generate a 10,000 ng/ml concentration $C1 \times V1 = C2 \times V2 \rightarrow 10{,}000\frac{ng}{ml} \times V1 = 20\frac{ng}{ml} \times 26\ ml$	1 ml per well, 6 wells, 4 plates plus waste: 24 + 1 ml Desired concentration: 150 ng/ml M-CSF Cytostock: Add 198 µl medium to 22 µl stock (50 ug/ml) to generate a 5,000 ng/ml concentration $C1 \times V1 = C2 \times V2 \rightarrow 5{,}000\frac{ng}{ml} \times V1 = 150\frac{ng}{ml} \times 25\ ml$

$V1 = \frac{20\frac{ng}{ml} \times 26\ ml}{10{,}000\frac{ng}{ml}} = 52\ ul$	$V1 = \frac{150\frac{ng}{ml} \times 25\ ml}{5{,}000\frac{ng}{ml}} = 750\ ul$
Cytostock: 1X is enough.	Cytostock: Make 4X: Add 198 µl medium to 22 µl stock (50 ug/ml) to generate a 5,000 ng/ml concentration Either: Mix the 220 from each in 1 tube and then transfer 750 µl to the 25 ml medium OR Transfer 187.5 µl from each to the 25 ml medium

Day 6 (Monday, week 2)

1. Heat up 52 ml medium

Gently remove 1 ml from cultures without touching the cells and replace with 1 ml medium containing 2x polarizing cytokines (see table above).

Day 7 (Tuesday, Week 2)

1. Heat up 245 ml medium

8 plates (4 donors X 2 (2 types of ECM))

- Remove PBS from ECM scaffolds.
- Add 1 ml medium and incubate at 37°C until cells are ready to be seeded on the scaffolds.
    - App. 70 ml cold medium needed
- Centrifuge the plate at 300g for 5 min at RT, discard supernatant.
- Add 1 ml PBS to each well and move the plate in figure eight
- Centrifuge the plate, discard supernatant
- Add 1 ml 1x trypLE to each well
- Incubate in 20 minutes (37°C)
- Detach cells by pipetting
- Harvest the cell suspension and pool each phenotype in 50 ml centrifuge tube

- Wash wells with 1 ml PBS and add to 50 ml centrifuge tubes.
- Inactivate trypLE by adding 13 ml fresh medium
- Centrifuge the tubes – 300g for 5 minutes and discard supernatant
- Resuspend pellet in 3.5 ml medium
- Count on nucleocounter
    - Add 200 µl medium to cell suspension, mix by gentle pipetting, and transfer 200 µl to eppendorf tube.
    - Make a dead count directly on suspension (nucleocassette). Note numbers in table below.
    - Transfer 100 µl cell suspension to new Eppendorf tube. Add 100 µl reagent A and mix. Add 100 reagent B. Count total cell number (nucleocassette)

Donor	Phenotype	Volume	Dead	Total	DF	Viable/ml Total * DF - Dead
B	M1	3.5 ml			3	
B	M2	3.5 ml			3	
C	M1	3.5 ml			3	
C	M2	3.5 ml			3	
D	M1	3.5 ml			3	
D	M2	3.5 ml			3	
F	M1	3.5 ml			3	
F	M2	3.5 ml			3	

- Adjust to a cell concentration of 2e5 cells/ml. If resulting volume is <3.3ml, then use cell suspension as is.

$$\frac{wanted\ cells\ \left(\frac{cells}{ml}\right)}{cell\ conc.\left(\frac{cells}{ml}\right)} x\ (3.5\ ml - 0.2ml) = total\ volume$$

$$Total\ volume - 3.3\ ml = Added\ medium$$

- Discard of medium from ECM scaffolds and seed 250 µl cell suspension in wells / 500 µl pr. well in control plates as illustrated below (Figures A1.2, A1.3, A1.4).

Overview of plates

Flow: **Microscopy**:

ASC ECM:

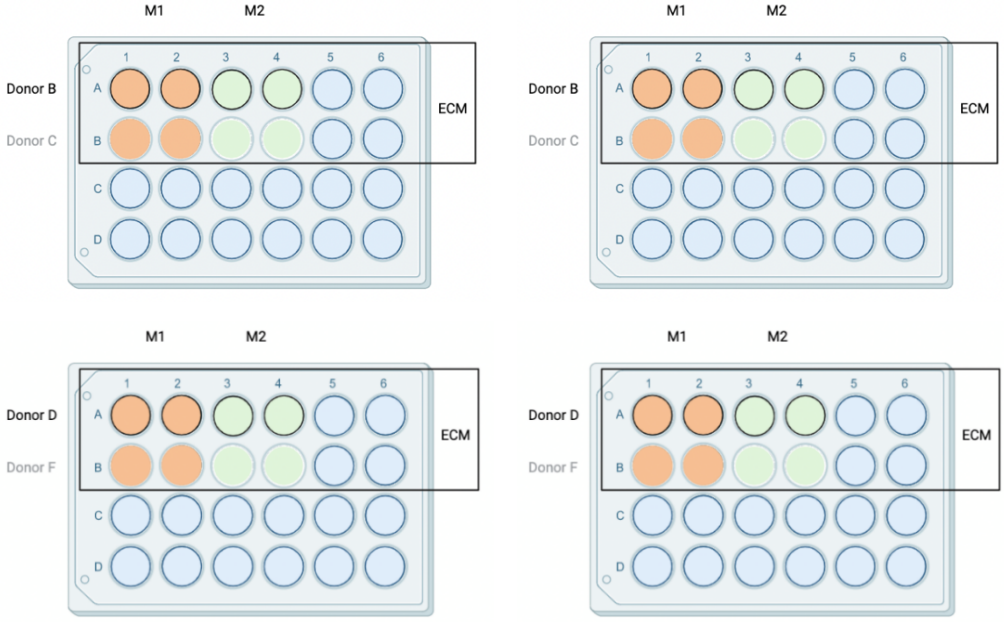

Fibro ECM:

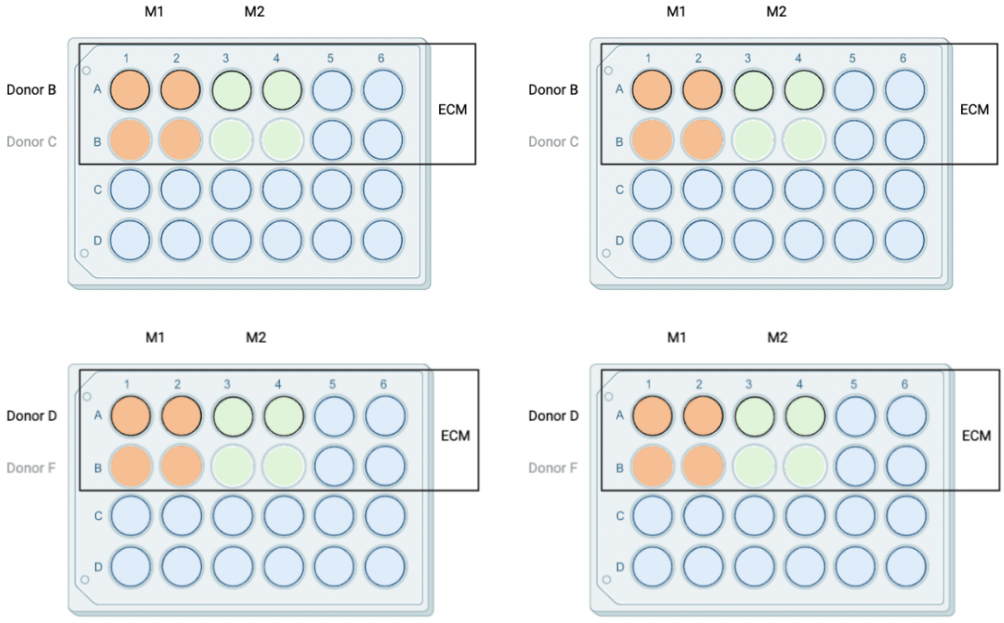

Control plates

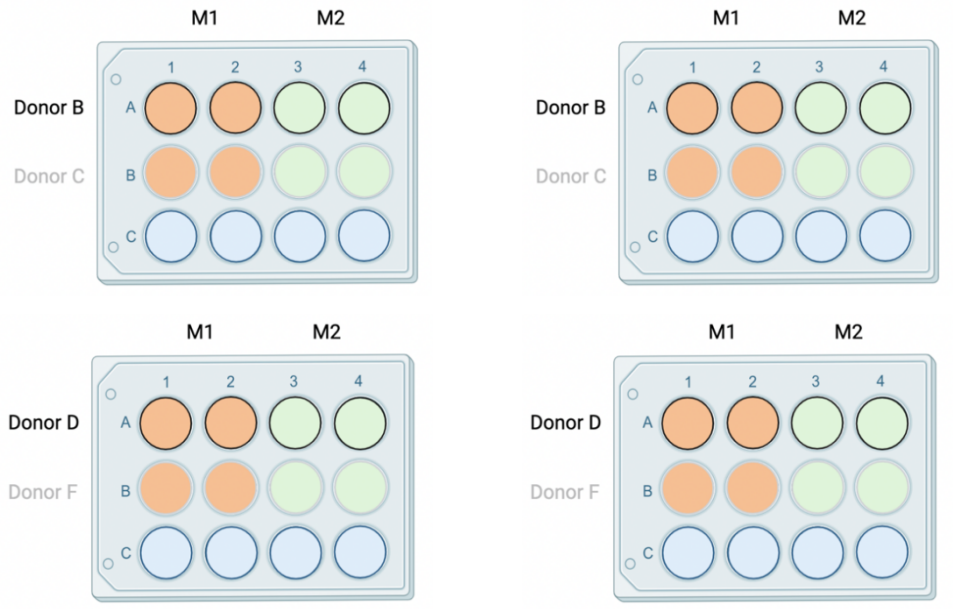

Add 500 µl 2x polarizing medium per well in 24 well plate / Add 1000 µl 2x polarizing medium per well in 12 well plate

M1	M2
0,5 ml per well in 24 well plates, 1 ml in 12 well plates plus waste: 32 ml + 3 ml =35 Desired concentration: 20 ng/ml GM-CSF Add 48 µl medium to 12 µl stock (50 ug/ml) to generate a 10,000 ng/ml concentration (x2) $C1 \times V1 = C2 \times V2 \rightarrow 10{,}000\frac{ng}{ml} \times V1 = 20\frac{ng}{ml} \times 35\ ml$ $V1 = \frac{20\frac{ng}{ml} \times 35\ ml}{10{,}000\frac{ng}{ml}} = 70\ ul$ add 70 µl to 35 ml medium	0,5 ml per well in 24 well plates, 1 ml in 12 well plates, plus waste: 32 + 3 ml = 35 Desired concentration: 150 ng/ml M-CSF Add 99 µl medium to 11 µl stock (50 ug/ml) to generate a 5,000 ng/ml concentration (x 10) $C1 \times V1 = C2 \times V2 \rightarrow 5{,}000\frac{ng}{ml} \times V1 = 150\frac{ng}{ml} \times 35\ ml$ $V1 = \frac{150\frac{ng}{ml} \times 35\ ml}{5{,}000\frac{ng}{ml}} = 1050\ ul$ add 1050 µl to 35 ml medium

Activation/Stimulation

There will be 4 phenotypes (Illustrated on figures below):

- Immature macrophages (M1 + M2)
- Mature macrophages (mM1 + M2c)

- To immature macrophages, add 250 µl medium pr. well / 500 µl pr. well in controls (12-well)

- To mature phenotypes (mM1 + M2c), add 250 µl 4x activating medium / 500 µl pr. well in controls (12-well plates). For **mM1**, the final concentration is **500 ng/ml LPS** and **5 ng/ml IFN-g**. For **M2c**, the final concentration is **40 ng/ml IL-10**. See procedure in table below

mature M1 (mM1)	M2c
LPS 0.25 ml per well in 24 well plate and 0.50 in 12 well plate, plus waste: 8 ml + 2 ml =10 ml Desired concentration: 2000 ng/ml Add 990 µl medium to 10 µl stock (5 mg/ml) to generate a 50,000 ng/ml concentration $C1 \times V1 = C2 \times V2 \rightarrow 50{,}000\frac{ng}{ml} \times V1 = 2000\frac{ng}{ml} \times 10\ ml$ $V1 = \frac{2000\frac{ng}{ml} \times 10\ ml}{50{,}000\frac{ng}{ml}} = 400\ ul$ To 10 ml medium, add 400 µl LPS **IFN-g** Add 450 µl medium to 50 µl stock (50 ug/ml) to generate a 5,000 ng/ml concentration Desired concentration: 20 ng/ml $C1 \times V1 = C2 \times V2 \rightarrow 5{,}000\frac{ng}{ml} \times V1 = 20\frac{ng}{ml} \times 10\ ml$ $V1 = \frac{20\frac{ng}{ml} \times 10\ ml}{5{,}000\frac{ng}{ml}} = 40\ ul$ To the LPS working solution, add 40 µl IFN-g	**IL-10** 0.25 ml per well in 24 well plate and 0.50 in 12 well plate, plus waste: 8 ml + 2 ml = 10 ml Desired concentration: 160 ng/ml Add 80 µl medium to 20 µl stock (50 ug/ml) to generate a 10,000 ng/ml concentration $C1 \times V1 = C2 \times V2 \rightarrow 10{,}000\frac{ng}{ml} \times V1 = 160\frac{ng}{ml} \times 10\ ml$ $V1 = \frac{160\frac{ng}{ml} \times 10\ ml}{10{,}000\frac{ng}{ml}} = 160\ ul$ To 10 ml medium, add 160 µl IL-10

Overview of plates

Flow: **Microscopy:**

ASC ECM:

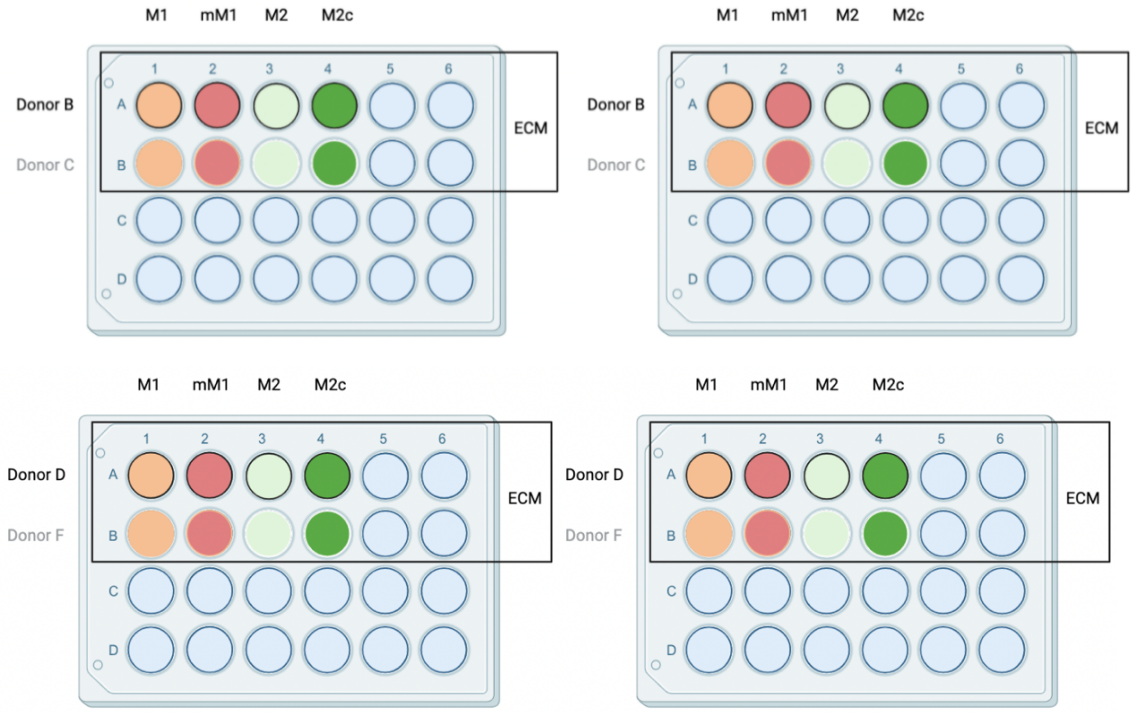

Fibro ECM:

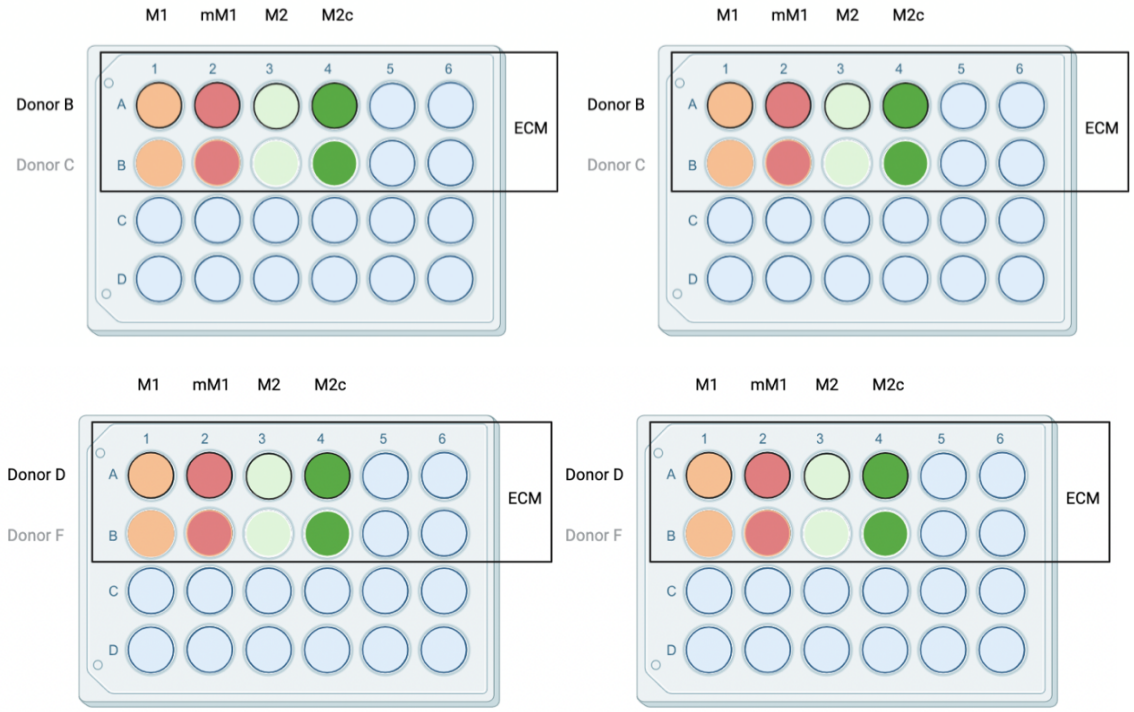

Control plade:

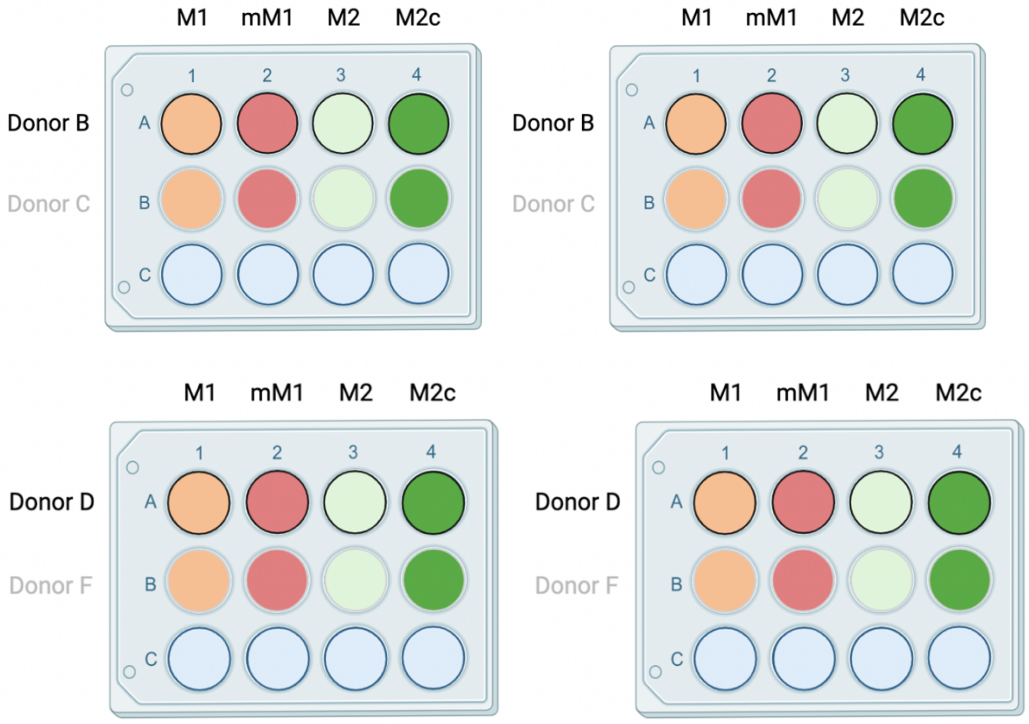

Day 9 (Thursday, Week 2)

Flow cytometry

Harvest cells:

1. Centrifuge plate at 300·g for 5 min. (A: 9, B: 5).
2. Save 80 µl medium in 96-well plates. Discard of the remaining medium and replace with 1 ml PBS. Incubate for 5 minutes at 37 °C.
3. Centrifuge plate at 300·g for 5 min. (A: 9, B: 5).
4. Add 1000 µl MACS buffer per well and refrigerate (4 °C) for 30 minutes.
5. After 30 minutes in the refrigerator with MACS buffer, harvest cells suspension and transfer cells to 50 ml centrifuge tube. (After havest of the first row à start incubation of next plate)
6. Add 1 ml PBS to each well
7. Thoroughly detach cells by pipetting and transfer harvested cells to the tube containing cells.
8. Fill tube with PBS to 15 mL, centrifuge 300·g for 5 min. and discard supernatant

9. Discard of supernatant. Resuspend in 400 µl (24 well plate) or 800 µl (12 well plate) PBS and transfer 2x200 µl to 96 well polypropylene plate as illustrated below (Figure A1.8).

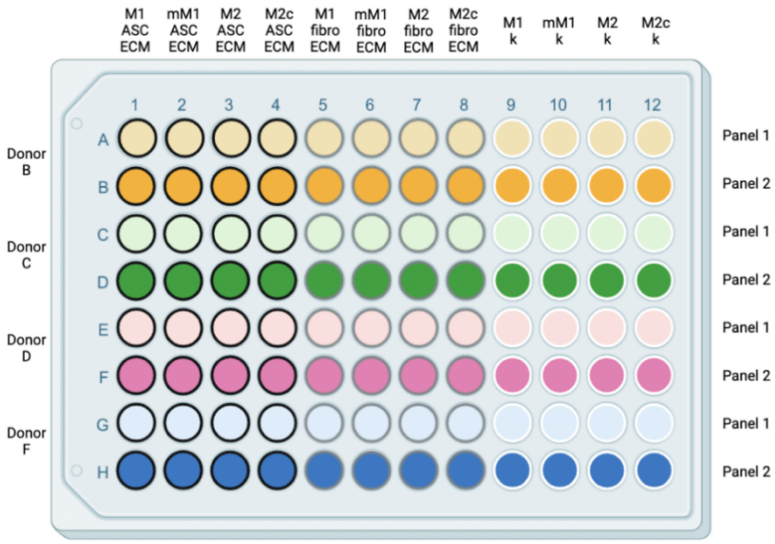

10. Centrifuge the plate at 300 x G for 5 min, discard supernatant
11. Agitate to dislodge pellet. Add 25 µl PBS to each well.

Viability stain and surface markers

12. Prepare 2x FVS780 working solution (1/4x manufacturers instruct)
    - For 96 wells ($96\ wells \cdot 25\ \mu l = 2.4\ ml$)
        i. 15 µl FVS780 stock
        ii. 3 ml Pbs
13. Add 25 µl FVS780 to all wells. Incubate for 15 minutes (4°C). Keep dark.
14. Add 100 µl FACS buffer to all wells. Centrifuge 300·g for 5 min. (4°C)
15. Discard of supernatants. Agitate plate to dislodge pellet.
16. Incubate stained wells with Fc Block

    96 wells (+4 loss), 25 ml each = 2.500 µl (2.5 ml)

    Working concentration: 10 ug/ml

    Stock: 0.5 mg/ml = 500 ug/ml

$$\frac{2.5\ ml \cdot 10\frac{\mu g}{ml}}{500\frac{\mu g}{ml}} = 0.05\ ml = 50\ \mu l$$

- 50 µl human FcBlock
- 2450 µl FACS buffer
- Vortex

17. Add 25 µl FcBlock working solution to all wells.
18. Incubate at 4°C for 10 min. In the meantime, prepare antibody master mix in Eppendorf or falcon tubes

Panel 1:

OBS a 2x working solution is generated, since Ab is diluted in cell solution.

Since 25 µl cells are seeded and only 25 µl antibody solution is added, the volume is divided by two below.

Antibody	Manufacturer instruct per test	Dilution	48 wells + 7 waste = 55 wells
CD1a	20 µl pr 100 µl à 10 µl per 50 µl	1/2x	*5µl x 55 = 275 µl*
DC-SIGN	20 µl pr 100 µl à 10 µl per 50 µl	1/4x	*2.5 µl x 55 = 137.5 µl*
CD14	5 µl pr 100 µl à 2.5 µl per 50 µl	1/2x	*1.25 µl x 55 = 68.75 µl*
HLA-DR	5 µl pr 100 µl à 2.5 µl per 50 µl	1/2x	*1.25 µl x 55 = 68.75 µl*
FACS buffer	55*25 µl = 1375 µl (total)	-	1375 µl - (275 µl + 137.5µl + 68.75 µl +68.75 µl) = 825 µl

Panel 2:

Antibody	Manufacturer instruct per test	Dilution	48 wells + 7 waste = 55 wells
CD38	5 µl pr 100 µl à 2.5 µl per 50 µl	1/2x	*1.25 µl x 55 = 68.75 µl*
ILT-4 (CD85d)	5 µl pr 100 µl à 2.5 µl per 50 µl	1/2x	*1.25 µl x 55 = 68.75 µl*
CD163	5 µl pr 100 µl à 2.5 µl per 50 µl	1x	*2.5 µl x 55 = 137.5 µl*
CD206	5 µl pr 100 µl à 2.5 µl per 50 µl	1/8x	*0.3125 µl x 55 = 17.1875 µl (17.19 µl)*
CD86	5 µl pr 100 µl à 2.5 µl per 50 µl	1/16x	*0.15625 µl x 55 = 8.59375 µl (8.59 µl)*
FACS buffer	55*25 µl = 1375 µl (total)	-	1375 - (68.75 µl - 68.75 µl - 137.5 µl - 17.19 µl - 8.59 µl) = 1074.22 µl

19. Add 25 µl Ab mix to stained wells. Incubate dark for 30 min at 4°C.
20. Add 100 µl FACS buffer per well and centrifuge at 300·g for 5 min. (4°C). Discard of supernatants. Agitate plate to dislodge pellet.
21. Add 200 µl FACS buffer per well and centrifuge at 300·g for 5 min. (4°C). Discard of supernatants. Agitate plate to dislodge pellet.

Fix/Perm

MOVE TO FUME HOOD

1. Resuspend thoroughly in 100 µl/well Cytofix/Cytoperm buffer, one row at a time using a multi-channel pipette, changing tips between rows.

1. Incubate for 20 min. at 4°C.
2. Add 100 µl Perm/Wash buffer per well and centrifuge at 300·g for 5 min. (4°C). Discard of supernatants in waste group H. Agitate plate to dislodge pellet (**on paper in fume hood**).
   FUME HOOD NOT REQUIRED BEYOND THIS POINT
3. Add 200 µl Perm/Wash buffer per well and centrifuge at 300·g for 5 min. (4°C). Discard of supernatants. Agitate plate to dislodge pellet.
   2. Add 200 µl Perm/Wash buffer per well and centrifuge at 300·g for 5 min. (4°C). Discard of supernatants. Agitate plate to dislodge pellet. Continue to intracellular staining.

Intracellular staining

22. Dilute antibody (CD68) in Perm/Wash buffer:

Antibody	Manufacturer instruct per test	Dilution	48 wells + 7 waste = 55 wells
CD68	5 µl pr 100 µl à 2.5 µl per 50 µl	1/2x	1.25 x 55 = 68.75 µl
Perm/wash buffer	55 x 50 µl = 2750 µl		2750 µl - 68.75 µl = 2681.25 µl

23. Add 50 µl Ab solution to cells in panel 1. Add 50 µl Perm/Wash buffer to cells in panel 2.
24. Incubate for 30 min (4°C).
25. Add 100 µl Perm/Wash buffer per well and centrifuge at 300·g for 5 min. (4°C). Discard of supernatants. Agitate plate to dislodge pellet.
26. Add 200 µl Perm/Wash buffer per well and centrifuge at 300·g for 5 min. (4°C). Discard of supernatants. Agitate plate to dislodge pellet.
27. Add 200 µl FACS buffer per well and store cold. Shield samples from light. Next day, analyze on FACSLyrics flow cytometer.

Fixation

Perform the complete procedure under a fume hood

- Discard of medium and wash all wells in 1 ml PBS.
- Fixate with paraformaldehyd
- Wash with PBS.
- Store in plastic bag at 4°C until staining

Picrosirius stain.

- Dilute HCL stock (1 mol/L) 1:100 in dH2O. Wash 1x 5 min with 0,01 M HCl
- Add 1 ml Picro-Sirius Red and incubate overnight (at room temperature) protected from light.
- Wash 1x 5 min with 0,01 M HCl
- Wash 1x with ddH2O (if the liquid remains yellow, wash 1x more with ddH2O)
- Perform microscopy